

BOLTED END PLATE BEAM TO COLUMN
CONNECTIONS UNDER EARTHQUAKE TYPE LOADING

A report
submitted in partial fulfilment
of the requirements for the degree of
Master of Engineering
at the
University of Canterbury,
Christchurch,
New Zealand.

by

N. D. Johnstone

February 1981

ABSTRACT

This thesis has tried to collate and compare the universally available design recommendations for this bolted end plate beam to column type of connection. Three specimens simulating these connections in a multistorey building were designed with the use of these recommendations and tested in an earthquake type loading situation. The results of these tests indicated that most of the design recommendations reviewed herein were valid.

ACKNOWLEDGEMENTS

I gratefully acknowledge the Heavy Engineering Research Association for their interest and financial support. I appreciate the generosity shown by Ajax GKN Limited for providing all the bolts used in the specimens and the test rig. I would also like to offer my thanks to the following people for their assistance during the course of this project;

Dr. W. R. Walpole, my supervisor, for his assistance and guidance throughout the project and also for his time and effort spent in designing and organising the construction of the test rig.

Ray Allen whose efforts and high quality of workmanship were invaluable in the construction of the test rig and in the testing of the specimens.

Professor I. R. Wood, acting head, and Professor R. Park, head of the Civil Engineering Department, for their interest and encouragement.

All those many other people who assisted in tasks ranging from sweating on the end of a hydraulic pump handle to typing this report. Their efforts are all appreciated.

TABLE OF CONTENTS

	<u>PAGE</u>
ABSTRACT	i
ACKNOWLEDGEMENTS	ii
TABLE OF CONTENTS	iii
LIST OF FIGURES	v
LIST OF TABLES	viii
NOTATION	ix

CHAPTERS

1	INTRODUCTION	1
2	THE SIMPLIFIED LOADING AND BEHAVIOUR OF THESE CONNECTIONS	2
3	A REVIEW OF LITERATURE ON THE DESIGN RECOMMENDATIONS FOR THESE CONNECTIONS	4
4	THE TESTS	12
	4.1 General Description of the Tests	12
	4.2 The design Procedure and Equations that were used	13
	4.3 Specimen One	16
	4.4 Specimen Two	18
	4.5 Specimen Three	20
	4.6 Measurements Recorded During the Tests	22
	4.7 Loads and Loading Sequence	22
5	RESULTS	35
	5.1 Specimen One	35
	5.2 Specimen Two	36
	5.3 Specimen Three	37

<u>CHAPTER</u>		<u>PAGE</u>
6	DISCUSSION	61
	6.1 Introduction	61
	6.2 Bolts	62
	6.3 End Plate	63
	6.4 Column Flanges	65
	6.5 General Discussion	67
7	RECOMMENDATIONS FOR FURTHER RESEARCH	69
8	CONCLUSIONS	70
	REFERENCES	71
	APPENDIX	73

LIST OF FIGURES

<u>FIGURE</u>		<u>PAGE</u>
2.1	General view of loads on this type of connection	3
3.1	Generally assumed deformation of the end plate	9
3.2	End plate dimensions	10
3.3	Yield line mechanism in end plate as suggested by Surtees and Mann ⁽¹⁰⁾	11
4.1	The specimen as part of a building	24
4.2	Plan of specimen, lateral bracing, dial gauges and load positions	25
4.3	Specimen one prior to testing	26
4.4	Shear forces in panel zone	27
4.5	Unstiffened column flange at the connection	28
4.6	Horizontal column flange stiffeners welded to flanges and web	28
4.7	Column flanges stiffened by the doubler plate welded to the column flange tips	28
4.8	Dimensions related to the unstiffened column flange capacity	29
4.9	Dimensions related to the column flange capacity when stiffened horizontally at the level of the beam flanges	29
4.10	Dimensions related to the column flange capacity when stiffened with doubler plates at the column flange tips	30
4.11	Yield line pattern of Fig. 4.9 when "C" is large	31
4.12	Details of specimen one	32
4.13	Details of specimen two	33
4.14	Details of specimen three	34

<u>FIGURE</u>		<u>PAGE</u>
5.1.1	Loading pattern, specimen one	40
5.1.2	Load versus deflection, beam "A", specimen one	41
5.1.3	Load versus deflection, beam "B", specimen one	42
5.1.4	Buckling of the beam flanges, specimen one	43
5.1.5	End plate of beam "B", specimen one, when $\mu = +4$, in the $\mu = 4$ cycle	44
5.1.6	End plate of beam "B", specimen one, when $\mu = +6.6$	44
5.1.7	Specimen one after testing	45
5.2.1	Loading pattern, specimen two	46
5.2.2	Load versus deflection, beam "A", specimen two	47
5.2.3	Load versus deflection, beam "B", specimen two	48
5.2.4	Buckling of the beam flanges, specimen two, after test	49
5.2.5	End plate of beam "B", specimen two, when $\mu = +6$	49
5.2.6	General view of specimen two after test	50
5.2.7	General view of specimen two at $\mu = -6$	50
5.3.1	Loading pattern, specimen three	51
5.3.2	Load versus deflection, beam "A", specimen three	52
5.3.3	Load versus deflection, beam "B", specimen three	53
5.3.4	End plate of beam "B", specimen two, when $\mu = +6$	54
5.3.5	General view of the connection, specimen three at $\mu = +6$	55
5.3.6	General view of the connection, specimen three, at $\mu = -7.5$	55
5.3.7	General view of the connection, specimen three, at $\mu = +10$	56
5.3.8	Close up view of the connection, specimen three, at $\mu = +10$	56
5.3.9	Fracture in the end plate of beam "B", specimen three	57

<u>FIGURE</u>		<u>PAGE</u>
5.3.10	Fracture in the end plate of beam "B" and some evidence of bending in double curvature in the end plate outstand, specimen three	57
5.3.11	Deformations of the column flange on the beam "A" side of specimen three	58
5.3.12	Deformation of the column flange on the beam "B" side and partial fracture between the column flange and doubler plate butt weld, specimen three	59
5.3.13	View of the panel zone where fracture has occurred over the full length between one of the column flanges and its doubler plate butt weld, specimen three	59
5.3.14	General view of specimen three after test showing additional beam lateral bracing c.f. Fig. 4.3	60

LIST OF TABLES

<u>TABLE</u>		<u>PAGE</u>
1(a)	Yield test results for specimens one and two	16
1(b)	Strengths of the components of specimen one in terms of the beam load	17
2	Strengths of the components of specimen two in terms of the beam load	19
3(a)	Yield test results for specimen three	20
3(b)	Strengths of the components of specimen three in terms of the beam load	21

NOTATION

A	=	Horizontal distance between the adjacent bolts on the end plate.
A_f	=	Area of beam flange.
A_w	=	Area of column web. (Depth of column section times its web thickness including doubler plates)
a	=	Vertical distance between the top or the bottom of the end plates and the adjacent bolt centres.
B	=	Width of the end plate.
b	=	Vertical distance between the edge of the beam flange weld and the adjacent bolt centres.
C	=	Vertical distance between the bolt centres immediately above and below a particular beam flange.
D	=	Bolt diameter.
D'	=	Bolt hole diameter.
d_b	=	Depth of beam.
d_f	=	Depth of beam between the flange centroids.
F	=	Tensile force per bolt.
$F_{mc}, F_{mb}, F_{ms}, F_{mp}, F_{mq}$	=	Column flange capacity for the beam tension flange force. The subscripts correspond to different column flange stiffening arrangements as described in Section 4.2.
f_{yc}, f_{yb}, f_{yp}	=	Yield stress in the column, beam, and end plate respectively.
k_c	=	$T_c + r_c$.
L	=	Length of yield line.
M	=	Plastic moment per unit length of yield line.
M_B	=	Plastic moment in the beam.
m	=	Horizontal distance between the bolt centre and the edge of the column flange root fillet.
n	=	Horizontal distance between the bolt centre and either the edge of the column flange or the face of the column flange tip stiffener whichever is applicable.
P_T	=	Tensile force per bolt (F).
P_{TB}	=	Effective force in the beam flange due to its plastic moment ($= \frac{M_B}{d_f}$)

P_{TC}	=	Effective force in the column flange due to its bending moment.
P_Y	=	Area of the column section times its yield stress.
Q	=	Prying force per bolt.
r_c	=	Radius of column web to flange fillet.
T_B	=	Beam flange thickness.
T_C	=	Column flange thickness.
T_P	=	Thickness of a panel zone doubler plate.
t	=	End plate thickness.
t_B	=	Beam web thickness.
t_c	=	Column web thickness.
V	=	Shear force corresponding to either the bolt or the panel zone.
V_b, V_c	=	Shear force in the beam and column respectively due to bending.
V_{ph}, V_{pv}	=	Shear forces in the panel zone in the horizontal and vertical directions respectively.
v	=	Vertical distance between the bolt centre and the edge of the adjacent horizontal column flange stiffener weld.
θ	=	Angle of plastic rotation in a yield line.
μ	=	Displacement ductility factor.

CHAPTER 1

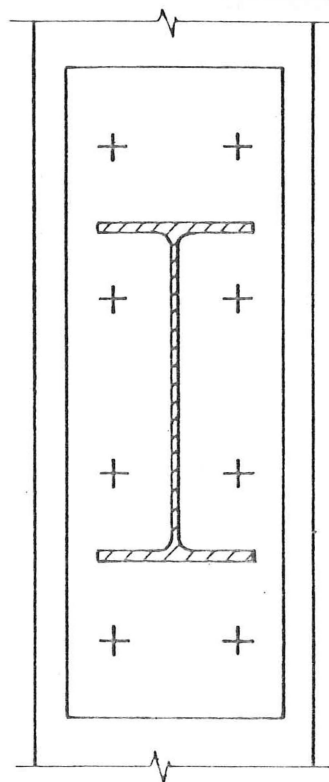
INTRODUCTION

Bolted end plate steel beam to column connections can facilitate quick structural erection and can provide reasonable strength, stiffness and ductile characteristics. In the past there has been a reasonable amount of research into the behaviour of these connections especially with respect to medium and smaller sized beam members in monotonically loaded situations. This thesis reviews and discusses past design recommendations for these connections. It also describes some tests which were carried out to determine the applicability of the above recommendations when these connections are subjected to earthquake type, cyclic racking, loads. The plastic design approach has been adopted here for assessing the strengths of the connections and their associated beams and columns.

CHAPTER 2

THE SIMPLIFIED LOADING AND BEHAVIOUR OF THESE CONNECTIONS

In the design of multistorey buildings to resist earthquake loads the general approach has included the over-design of the columns and the beam to column connections. The purpose of this has been to discourage the formation of plastic hinges in the column and in the beam to column connections and to also reduce the likelihood of a brittle type failure occurring in the connections. To design the connection the beam and column moments and forces were assumed to generally act on the connection as follows. The column and beam moments were resolved into parallel forces, one in each flange as shown in Fig. 2.1. The beam tension flange force was transferred into the column flange by way of the end plate and the immediately adjacent bolts. The beam compression flange force was transferred by direct bearing between the end plate and the column. Vertical shear was transferred across the connection through the bolts in bearing and/or through direct friction between the end plate and the column flange. This latter component has been often conservatively ignored.



VIEW X-X

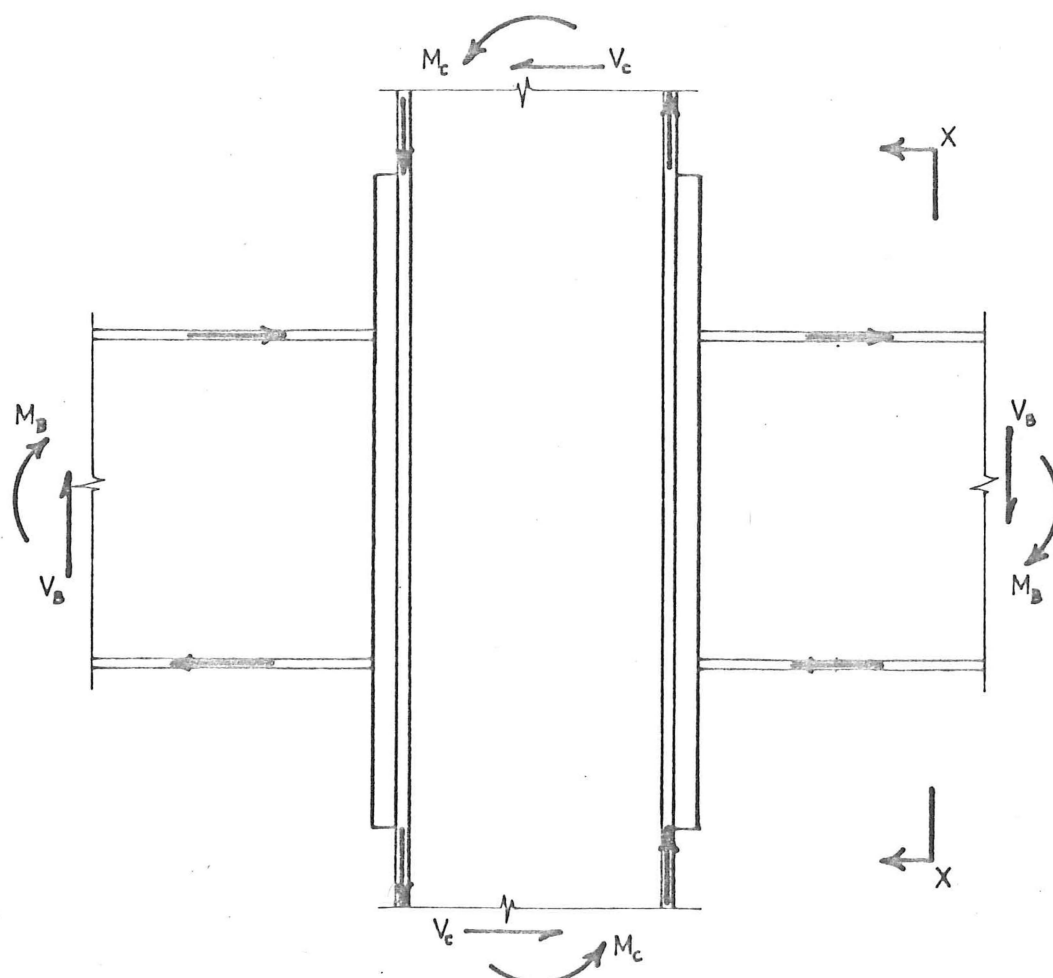


FIG. 2.1 General view of the earthquake loads on this type of connection.

CHAPTER 3

A REVIEW OF LITERATURE ON THE DESIGN

RECOMMENDATIONS FOR THESE CONNECTIONS

There are several published articles related to this type of connection and in general their recommendations have become less conservative as research has progressed. In a fundamental sense the currently accepted design procedure for these connections is:

- (1) Calculate or assume the magnitude of the bolt prying effects.
- (2) Calculate the bolt size.
- (3) Calculate the end plate dimensions.
- (4) Design the beam to end plate welds.
- (5) Determine the column flange and web stiffening requirements.

These five aspects are interdependent and design methods make some allowance for this. Some particularly prominent published articles on this type of connection design are reviewed in the following paragraphs.

Sherbourne⁽⁵⁾ 1961, was one of the earlier researchers to collate existing knowledge and present a design method for this type of connection. He also tested five connections of this type to study their behaviour. Unlike all of the following authors he used a smaller tension flange force in his design recommendations, i.e. $P_{TB} = A_f \times f_{yb}$ rather than the more commonly assumed force of $P_{TB} = \frac{M_B}{d_f}$. Sherbourne assumed that the beam tension flange force was carried equally between all the bolts both immediately above and below that flange. That assumption was common to all of the following published articles. He did not explicitly include the additional tension in the bolts due to prying but did seem to make some allowance by using the bolt proof stress rather than the ultimate stress, to work out the bolt size required. He assumed that the end plate acted in double curvature, as shown in Fig. 3.1, with plastic moments occurring in it at both the horizontal line of the bolt centres and the centre of the beam tension flange. To calculate the magnitude of the plastic moment he used Von Mises yield criteria to allow for the weakening effect of shear when acting in conjunction with bending in the end plate. Sherbourne also presented

some equations for assessing the need of column web stiffening to prevent its buckling near the beam compression flange. These equations were relatively complex and do not appear to have been used by the following authors reviewed here.

The A.S.C.E. Manual No.41⁽⁴⁾, 1971, presented a design method for these connections. It was largely collated from previous work. To assess the loads on the bolts the manual gave a simple approximate equation for calculating the bolt prying force, i.e.

$$Q = \left(\frac{3b}{8a} - \frac{t^3}{20} \right) \times F$$

see Fig. 3.2 where in this equation "t" is in inches. This is a simplified form of the equation recommended by Douty and McGuire.⁽⁸⁾ The Manual suggested that some or all of the shear in the joint would be carried by friction and could be calculated from the bolt pre-load and the friction coefficient. The Manual assumed that the end plate acted in double curvature, as shown in Fig. 3.1, with plastic moments occurring in it at both the horizontal line of the bolts and the face of the beam tension flange. In the derivation of the end plate thickness equation it seemed to gain a factor of two with its end plate width term, "B", i.e. it gave,

$$t = \left(\frac{M_B \times b}{d_b \times \frac{B}{2} \times f_{yp}} \right)^{\frac{1}{2}}$$

but this should perhaps have been,

$$t = \left(\frac{M_B \times b}{d_b \times B \times f_{yp}} \right)^{\frac{1}{2}}$$

This latter equation is similar to that given by Mann and Morris.⁽¹⁾

Grundy et al⁽⁶⁾, 1977, collated a design procedure from existing literature and from some of their own work. They also performed two tests to study the behaviour of these connections. Grundy et al recommended a 20% increase in the bolt design load to allow for prying effects. Unlike the other articles reviewed here they suggested that eight bolts per beam flange could be used although with the proviso that a horizontal column flange stiffener is used. They assumed that the tension flange force would be shared equally among that group of eight bolts. They recommended that the vertical shear in the connection could be carried solely or predominantly by the compression flange bolts. They assumed that the end plate acted in double curvature, see Fig. 3.1, and they used the allowable stress method to obtain the end plate equation,

$$t = \left(\frac{2 M_B \times b}{d_f \times f_{yp} \times B} \right)^{\frac{1}{2}}$$

where in this case " M_B " was the unfactored beam moment, i.e. the working beam moment. This equation was approximately 20% more conservative than that used by Mann and Morris⁽¹⁾ and by Hogan and Thomas.⁽⁷⁾ Grundy et al provided equations for calculating the capacity of the column flange to resist the load of the beam tension flange bolts. These equations appear to be approximately 50% more conservative than those proposed by Packer and Morris.⁽²⁾ Grundy et al did include in their equations the weakening effect of other column flange stresses due to column axial load and bending. This was not done by Packer and Morris.

Hogan and Thomas⁽⁷⁾, 1978, collated previous recommendations for this type of connection and then presented a design method. From the work of Gorenc and Tinyou⁽¹⁸⁾ they recommended a maximum prying force of 20% for when the end plate thickness, " t ", was greater than 1.4 times the bolt diameter, " D ". They also quoted some more elaborate equations for calculating bolt prying effects. They assumed that the shear in the connection was carried equally by all the bolts. They assumed that the end plate acted in double curvature with plastic hinges forming in it at the face of the beam tension flange and along the horizontal line of the bolt centres. This lead to their recommendation of the end plate equation,

$$t = \left(\frac{M_B \times b}{d_f \times f_{yp} \times B} \right)^{\frac{1}{2}}$$

Hogan and Thomas presented some equations for calculating both the stiffened and unstiffened capacities of the column web and flange in the connection region. For the column web they recommended that $f_{yc} \times t_c (T_B + 5k_c + 2t) \geq P_{TB}$. For the column flange capacity in the beam tension flange region their recommended equations tend to be more conservative than those proposed by Packer and Morris⁽²⁾ but not as conservative as those proposed by Grundy et al.⁽⁶⁾

Packer and Morris⁽²⁾, 1977, carried out some research into the failure mechanisms of both the end plate and the column flanges in the beam tension flange region of the connection. In their research they used yield line theory as a basis for their analyses. They subsequently recommended a design procedure for this type of connection. They recommended a $33\frac{1}{3}\%$ increase in the bolt's design tensile load to allow for prying effects as proposed by Surtees and Mann.⁽¹⁰⁾ Like many of the previous articles reviewed here they assumed that the end plate acted in double curvature with plastic hinges

forming in it at the face of the beam tension flange and on the horizontal line of the bolt centres. Refer to Fig. 3.1. In their end plate equation they made some allowance for the reduced section affected by the presence of the bolt holes, i.e.,

$$t = \left(\frac{M_B \times b}{d_f \times f_{yp} \times (B - D')} \right)^{\frac{1}{2}}$$

They recommended some equations for assessing the column flange capacity in the beam tension flange region. These were for both unstiffened and stiffened column flanges where in the latter case the stiffening was provided by full depth horizontal plate stiffeners. Their equations didn't take into account the weakening effect of other stresses in the column flanges due to column axial load and bending. Their equations for the column flange capacities are less conservative than those proposed by Hogan and Thomas⁽⁷⁾ and Grundy et al.⁽⁶⁾

Mann and Morris⁽¹⁾, 1979, appear to have largely based their paper on that of Packer and Morris⁽²⁾, although with some modification. They recommended a $33\frac{1}{3}\%$ increase in the bolt's design tensile load to allow for prying effects as proposed by Surtees and Mann.⁽¹⁰⁾ They also recommended that the edge distance, "a", should not be less than 2.5 times the bolt diameter, "D", to keep prying effects at a realistic level. To calculate the end plate dimensions they recommended the equation,

$$t = \left(\frac{M_B \times b}{d_f \times f_{yp} \times B} \right)^{\frac{1}{2}}$$

This is slightly different from that recommended by Packer and Morris. Mann and Morris reasoned that the work done in deforming the bolts compensated for the loss of end plate strength that was due to the existence of the bolt holes. They recommended the use of fillet welds to join the beam onto the end plate. This was to reduce both the risk of lamellar tearing and the preparation costs. They recommended a simple design rule which was that the throat thickness be not less than $0.5 \times T_b$ for the flange welds and $0.5 \times t_b$ for the web welds, provided that the heavier flange weld was continued down the web on the tension side for at least 50 mm. This provision was to prevent tension cracking of the weld in the root fillet. For assessing the column flange adequacy in the beam tension flange region they recommended the formulae proposed by Packer and Morris although for a different form of column flange stiffening they also presented some of the work done by

Zoetemeijer⁽¹¹⁾ with respect to using column flange doubler plates. To determine the need and extent of column web stiffening in the beam compression flange zone they quoted some equations from the European recommendations¹², and from Mann.⁽¹³⁾

Surtees and Mann⁽¹⁰⁾, 1970, carried out research into the failure mechanism of the end plates. They recommended that the load on any one of the four tension bolts be calculated from,

$$F = \frac{M_B}{3 \times d_f} .$$

This allowed an additional $33\frac{1}{3}\%$ increase in the design tensile load of the bolts to allow for prying effects. They recommended that the end plate dimensions be calculated from the following equation,

$$T = \left(\frac{M_B}{d_f \left(\frac{2B}{C} + \frac{d_f}{A} \right) \times f_{yp}} \right)^{\frac{1}{2}}$$

This took into account the additional strength that was given to the end plate by the restraining action of the attached beam web. Refer to Fig. 3.3. It is subsequently the least conservative of all the end plate thickness equations that are reviewed here.

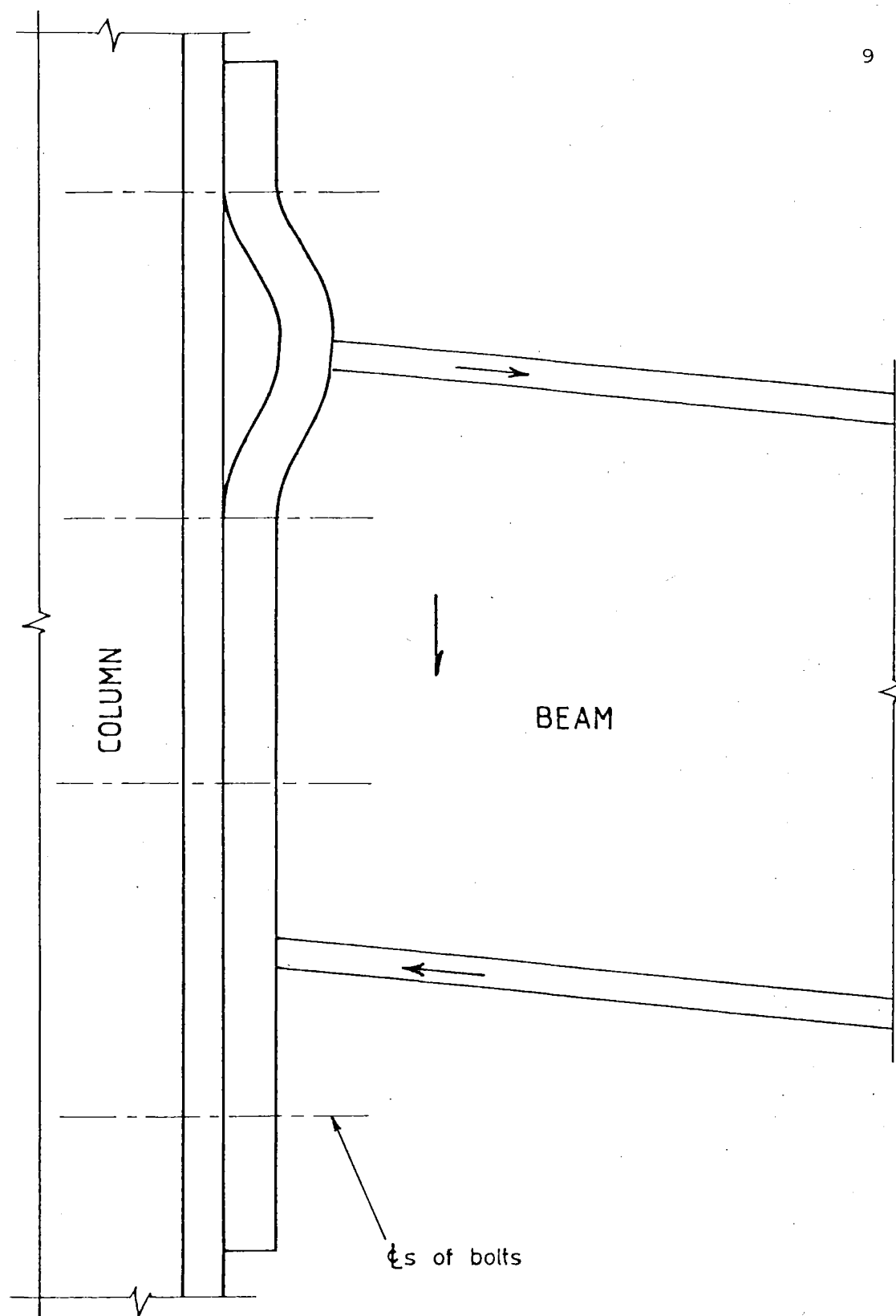
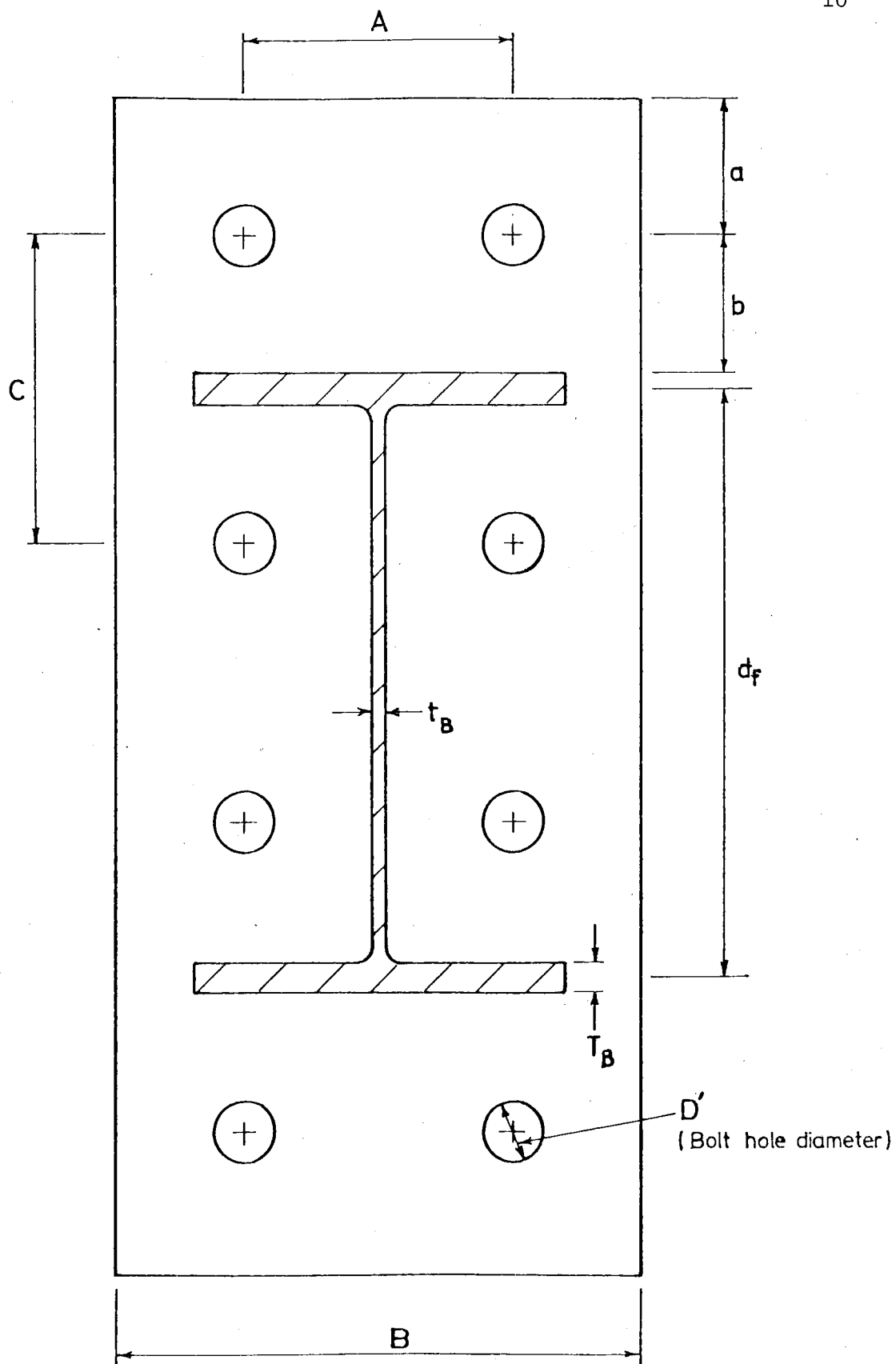


FIG. 3.1 Generally assumed deformation of the end plate.



End plate thickness = t

FIG. 3.2 End plate dimensions.

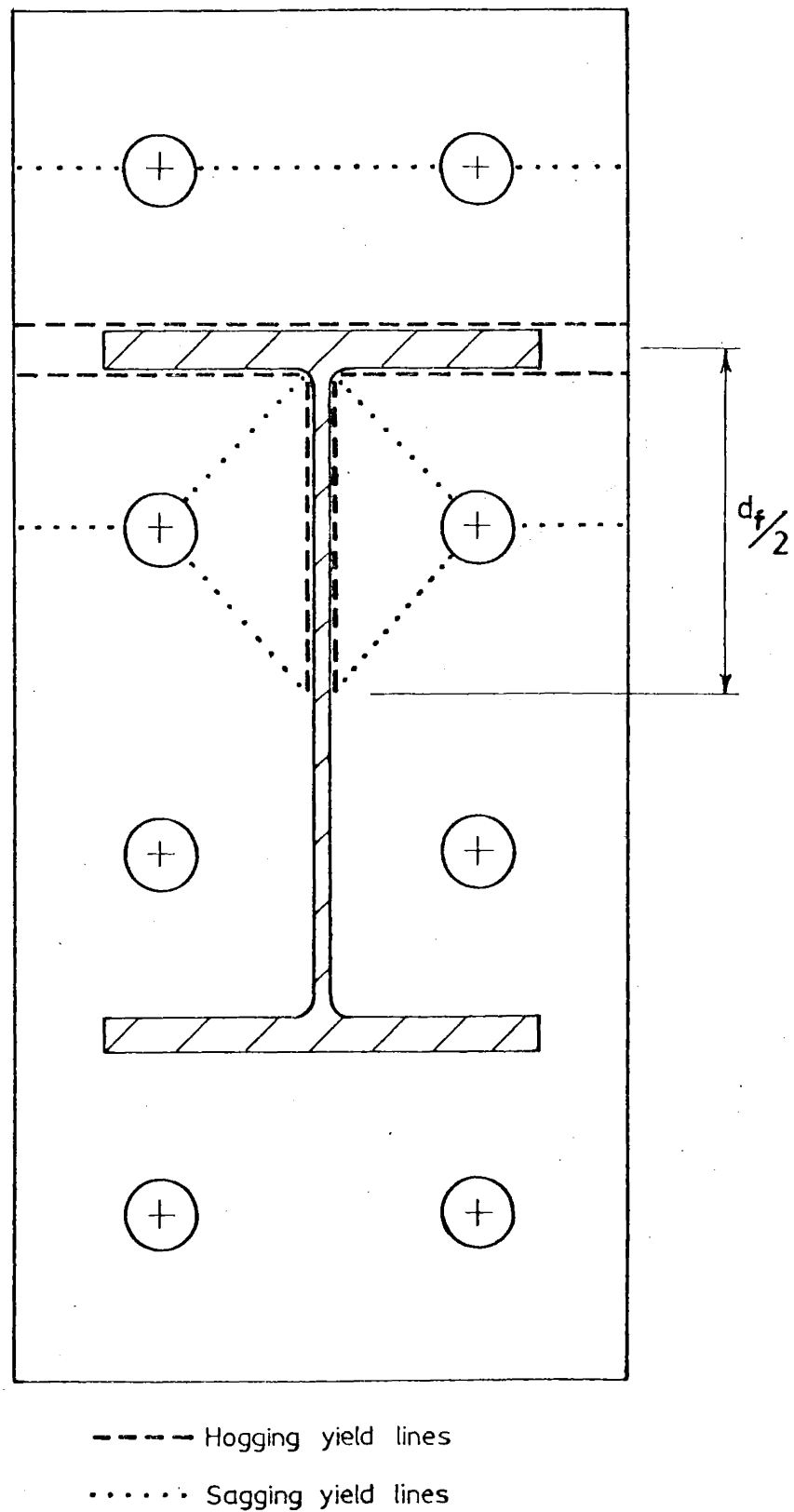


FIG. 3.3 Yield line mechanism in the end plate as suggested by Surtees and Mann⁽¹⁰⁾

CHAPTER 4

THE TESTS

4.1 GENERAL DESCRIPTION OF THE TESTS

The form of the experiment was chosen so as to be reasonably representative of a one way beam to column connection in a multi-storey building when under earthquake cyclic loading conditions as shown in Fig. 4.1. In practice the relative beam and column sizes, their spacing, loads and degree of bracing may all differ significantly from those tested here. The flexibility of the specimens tested exceeded the code limits⁽²¹⁾, however their general behaviour would have been very similar.

The N.Z.S. 3404 1977⁽¹⁶⁾ Section 12.4.7 requires that the columns be overdesigned to discourage the formation of plastic hinges in them. This was subsequently done as indicated by the design loads which are detailed in later sections of this chapter.

The N.Z.S. 3404 1977 also requires that the connection be overdesigned to allow for moment gradient and strain hardening effects in the beams. To allow for this a 25% increase in the plastic moment of the beams was allowed for when designing the connection of specimens one and two. The connection of specimen three was under designed so that its behaviour could be studied more closely at ultimate load and failure.

Mild steel with a specified yield stress of 250 MPa was used in the fabrication of all parts of the specimens except for the use of H.S. bolts. These bolts were assumed to be acting in a bearing type joint and were chosen in accordance with the requirements of the A.S.1511 - 1973.⁽¹⁷⁾ The part turn method was used when the bolts were tightened. In all three of the specimens tested here this meant that the bolts were tightened by a half turn of the nut from the snug tight position. Standard washers were placed under both the head and nut of the bolts.

The specimens were set up in the test rig as indicated on Fig's 4.2 and 4.3. The beam loads were applied at their ends by means of a hydraulic jack through a tie rod system. The column axial compression load was applied by two hydraulic jacks, in parallel, and four macalloy bars. The latter were symmetrically located around the column section and transferred the column compression load reactions between its ends. This self supporting axial load system did not allow P-delta effects to be generated from relative interstorey lateral displacements as indicated in Fig. 4.1. This figure compares the test situation with the real situation. The beam points of contraflexure are displaced under point loads instead of the column swaying. The situation at the joint is quite similar but the absence of the column P-delta effect would change the stresses to some extent in the column and in the column section of the connection.

Shims were placed in the connection between the end plate and the column flange. These are commonly used in practice to overcome tolerance problems during erection. In the tests here they also helped to discern between the column flange and the end plate deformations as can be seen in Fig's 5.1.5, 5.1.6 and 5.2.5.

Before the specimens were tested their connection regions were painted with a white plaster solution. This was intended to reveal the occurrence and location of yielding.

4.2 THE DESIGN PROCEDURE AND EQUATIONS THAT WERE USED

The beam size used, 310 UB46, was common to all the tests. The column size was chosen so that it could support the required beam moments plus a reasonable axial compressive load. The column size was generally chosen to comply with the following two equations;

$$(1) \quad M_{pc} = 1.18 \left(1 - \frac{P}{P_y}\right) \times M_p$$

from 10.5.2 of AS1250-1975⁽¹⁹⁾

(2) The formula for the reduced plastic moduli when under axial load. From page 40 of AISC Tables.⁽²⁰⁾

The capacity of the column flange to resist the tension bolt forces was also considered when making the choice of column size. Equations relating to this are given later on in this section. Other column design criteria in NZS 3404⁽¹⁶⁾ were not critical here.

The tensile load in each bolt was calculated using the equation recommended by Surtees and Mann⁽¹⁰⁾,

$$F = \frac{M_B}{3 \times d_f}$$

The beam shear force was assumed to be carried equally by all eight bolts in the connection. The effect of shear in the bolts was checked using the equation,

$$\left(\frac{P_t}{P_{to}} \right)^2 + \left(\frac{V}{V_{ob}} \right)^2 \leq 1.0 \quad (\text{from AS 1511 - 1973}^{(17)})$$

and was found to be minimal. The values of P_{to} and V_{ob} used were derived from the maximum permissible applied loads given in AS 1511 when multiplied by a 1/0.6 factor which is given in the AS 1250 - 1975.⁽¹⁹⁾

The end plate dimensions were calculated using the equation recommended by both Mann and Morris⁽¹⁾ and Hogan and Thomas.⁽⁷⁾

$$t = \left(\frac{M_B \times b}{d_f \times f_{yp} \times B} \right)^{\frac{1}{2}}$$

The shear forces and column axial forces in the panel zone were calculated, see Fig. 4.4, and then column web doubler plates were added so that the following equation was satisfied,

$$\left(\frac{P}{A_s f_y} \right)^2 + \left(\frac{V}{0.55 A_w f_y} \right)^2 \leq 1.0$$

(from Section 12.4.9 of N.Z.S. 3404⁽¹⁶⁾).

The column web was also checked for buckling in the beam compression flange region by using the equation recommended by Hogan and Thomas.⁽⁷⁾

$$P_{TB} \leq f_{yc} \times t_c (T_B + 5 k_c + 2t).$$

The column flange capacities in the beam tension flange region were calculated from both the equations recommended by Packer and Morris⁽²⁾ and from some other equations derived by the author for the situation when the column web doubler plates are welded to the column flange tips. The capacity of the unstiffened column flange, as shown in Fig. 4.5, was given by Packer and Morris as being the larger of the forces that are calculated from the following two equations;

$$(i) \quad F_{mc} = T_c^2 \times f_{yc} \left[3.14 + \frac{(2n + C - D')}{m} \right]$$

(where failure will occur by yielding in the column flanges)

Refer to Fig. 4.8.

$$(ii) \quad F_{mb} = T_c^2 \times f_{yc} \left[3.14 + \frac{0.5 \times C}{m + n} \right] + \left[\frac{2 B_u \times n}{m + n} \right]$$

(where failure will occur by fracture of the bolts)

Refer to Fig. 4.8.

The capacity of the column flange as stiffened in Fig. 4.6 was calculated from the equation recommended by Packer and Morris,

$$F_{ms} = T_c^2 \times f_{yc} \left[\left(\frac{1}{v} + \frac{1}{w} \right) (2m + 2n - D') + \left(\frac{2v + 2w - D'}{m} \right) \right]$$

where $w = (m(m+n - 0.5 D'))^{\frac{1}{2}}$. Refer to Fig. 4.9.

The capacity of the column flange when stiffened with the a panel zone doubler plate which was butt welded to the column flange tips was calculated from the following equation,

$$F_{mp} = T_c^2 \times f_{yc} \left[\frac{3m + 3n - D'}{2g} + \frac{3g + 2C - 1.5 D'}{2m} + \frac{g(1+2r) + (1+r) C - 1.5 D'}{2n} \right]$$

where

$$g = \left[\frac{m n (3m + 3n - D')}{3n + (1+2r)m} \right]^{\frac{1}{2}}$$

Refer to Fig. 4.10.

The derivation for this equation is given in the appendix.

If the vertical distance between the adjacent bolts, "C", became too large then individual mechanisms would occur around each of the bolts giving a lower collapse load, F_{mq} , than that given by F_{mp} . Refer to Fig. 4.11.

$$F_{mq} = 2T_c^2 f_{yc} \left[\frac{2m + 2n - D'}{g} + \frac{2g - 0.5 D'}{m} + \frac{2g - 0.5 D'}{n} \right]$$

where "g" is the same as for F_{mp} . See appendix also for the derivation of this equation.

4.3 SPECIMEN ONE

It was intended in this specimen to over-design the column by 25% and the connection by 25%. The beam and column sizes chosen were 310 UB 46 and 250 UC 89 respectively. Details of the specimen can be seen in Fig. 4.12. Standard⁽²²⁾ yield tests were carried out on the component parts of the specimen and the results are given in Table 1(a) below.

TABLE 1(a)

Component Tested	Yield Stress (MPa)
Beam	289
Column	300
End plate	298
Panel zone doubler plate	241

The strengths of the components of the specimen were calculated for both of the following situations,

- (1) The initially assumed dimensions and yield stresses, nominal 250 MPa.
- (2) The actual dimensions and yield stresses of the connection and components respectively. These dimensions were measured prior to the testing and the yield stresses were determined from yield tests on offcuts of the fabricated specimens.

These strengths were then related to the beam loads and are shown in Table 1(b).

TABLE 1(b)

Component	Load required on end of beam to reach the strength capacity of the corresponding component (kN).	
	When calculated using specified yield stresses and the dimensions shown in Fig. 4.12.	When calculated with the measured dimensions and actual yield stresses.
Beam (plastic moment)	67.0	77.5
Column (axial load of 1300 kN with reduced plastic moment)	74.2	100.5
M30.H.S. Bolts (assuming 33% prying)	106.0	-
End plate ^(1 & 7)		
$t = \left(\frac{M_B \times b}{d_f \times f_{yp} \times B} \right)^{\frac{1}{2}}$	84.9	106.8
End plate ⁽¹⁰⁾		
$t = \left(\frac{M_B}{d_f \times f_{yp} \left(\frac{2B}{C} + \frac{d_f}{A} \right)} \right)^{\frac{1}{2}}$	138.0	164.5
Panel zone in shear (when column axial load = 1300 kN)	87.4	89.5
Column flange capacity	85.0	100.7

The column axial load used gave $P/P_y = 0.38$ where P_y was calculated from the actual yield stress. Some difficulties were experienced during the fabrication of this specimen because of welding distortions. The first distortions occurred when the doubler plates, welded to each side of the column web, pulled the column flanges inwards. This resulted in the column flanges being convex across their column faces. To remove this physical distortion the column was suitably heated, straightened and allowed to cool slowly to minimise the likelihood of altering the physical properties of the steel. The second set of distortions occurred when the column flanges were locally deformed by the column flange stiffeners pulling them inwards. Details of the connection and the welds can be seen in Fig. 4.12.

4.4 SPECIMEN TWO

This specimen was identical to specimen one except for two variations in their fabrication. In specimen two the panel zone doubler plates were butt welded to the column flange tips and the beams were fillet welded to the end plates as recommended by Mann and Morris⁽¹⁾ and shown in Fig. 4.13. Yield stresses for the component parts are as given for specimen one in Table 1(a). The strength of the components of the specimen were calculated and are presented in Table 2.

TABLE 2.

Component	Load required on end of beam to reach the strength capacity of the corresponding component (kN).	
	When calculated using specified yield stresses and the dimensions shown in Fig. 4.13.	When calculated with the measured dimensions and actual yield stresses
Beam (plastic moment)	67.0	77.5
Column (axial load of 1300 kN with reduced plastic moment).	74.2	100.5
M30 H.S. Bolts (assuming 33% prying)	106.0	-
End plate ^(1 & 7)	97.2	119.3
$t = \left(\frac{M_B \times b}{d_f \times f_{yp} \times B} \right)^{\frac{1}{2}}$		
End plate ⁽¹⁰⁾	138.0	164.5
$t = \left(\frac{M_B}{d_f \times f_{yp} \left(\frac{2B}{c} + \frac{d_f}{a} \right)} \right)^{\frac{1}{2}}$		
Panel zone in shear (when column axial load = 1300 kN)	87.4	89.5
Column flange capacity	94.7	113.6

The column axial load used gave $P/P_y = 0.38$ where P_y was calculated from the actual yield stress.

4.5 SPECIMEN THREE

In this specimen the connection was under designed so that its behaviour and failure could be studied more closely. The column was over designed by about 25% to prevent failure by plastic hinge action in the column. The beam and column sizes chosen were 310 UB 46 and 250 UC 73 respectively. Details of the specimen can be seen in Fig. 4.14. Yield tests were carried out on the component parts of the specimen and the results are given in Table 3(a).

TABLE 3(a)

Component Tested	Yield Stress (MPa)
Beam	293
Column	338
End plate	261
Panel zone doubler plate	249

The strengths of the components of the specimen were calculated and are presented in Table 3(b).

TABLE 3(b)

Component	Load required on end of beam to reach the strength capacity of the corresponding component (kN).	
	When calculated using specified yield stresses and the dimensions shown in Fig. 4.14.	When calculated with the measured dimensions and actual yield stresses
Beam (plastic moment)	66.7	77.2
Column (axial load of 1440 kN with reduced plastic moment)	41.9	79.7
M24 H.S. Bolts (assuming 33% prying)	66.3	-
End plate ^(1 & 7)		
$t = \left(\frac{M_B \times b}{d_f \times f_{yp} \times B} \right)^{\frac{1}{2}}$	53.1	65.6 (beam "A") 77.9 (beam "B")
End plate ⁽¹⁰⁾		
$t = \left(\frac{M_B}{d_f \times f_{yp} \left(\frac{2B}{C} + \frac{d_f}{A} \right)} \right)^{\frac{1}{2}}$	71.7	74.8
Panel zone in shear (when column axial load = 1440 kN)	59.3	68.5
Column flange capacity	46.7	63.2

The column axial load used gave $\frac{P}{P_y} = 0.46$ where P_y was calculated from the actual yield stress.

The butt welds between the end plate and the beams were splayed out by different amounts resulting in a smaller value of "b" for beam "B" than for beam "A". Hence the two different values for the end plate capacity^(1&7) in the right hand column of Table 3(b).

4.6 MEASUREMENTS RECORDED DURING THE TESTS

Measurements were taken at intervals throughout the tests to monitor the load deformation characteristics. This entailed:

- (1) Regular measurement of loads and deflections at the ends of the beams during the cyclic loading pattern.
- (2) Regular measurement of the column axial load to ensure that it was maintained.
- (3) Measurement at the zero and maximum load points of each cycle with an array of displacement (dial) gauges and strain (staeger) gauges. These were intended to monitor the column and beam flexure and the panel zone shear, end plate and column flange deformations.

The positions of the dial gauges and loading points are shown in Fig. 4.2. In the panel zone the staeger gauges were arranged in a diamond pattern so that the principle stresses could be analysed. On the beam and column flanges some staeger gauges were aligned longitudinally to monitor the bending and axial deformations of those members.

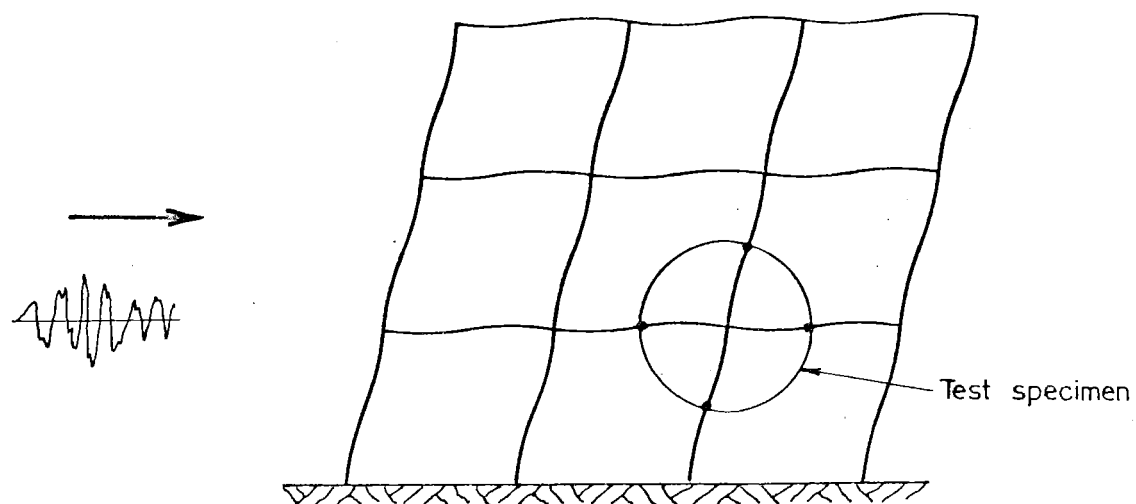
4.7 LOADS AND LOADING SEQUENCE

The maximum beam loads for the first load cycle were chosen so that a displacement ductility factor, " μ ", of magnitude 0.75 would be just reached. This enabled a displacement to be calculated for when $\mu = 1.00$, i.e. 1.333 times the displacement at μ equals 0.75. After this first loading cycle on each specimen the following load cycles were performed with the displacement as the controlling variable. The displacements were measured at A1 and B1, Refer to Fig. 4.2.

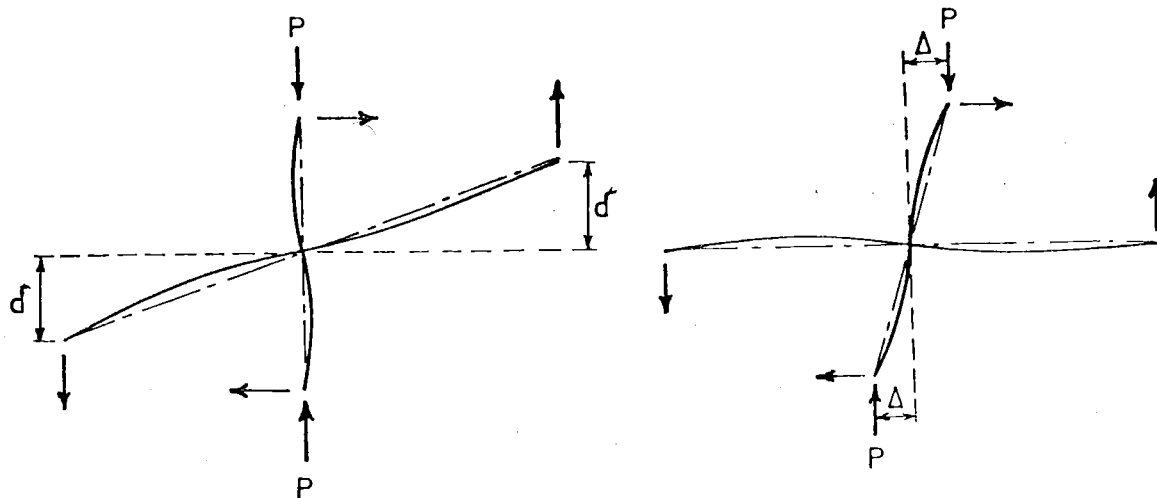
In specimens one and two the load associated with $\mu = 0.75$ (58.1 kN) was assumed to be the load that would cause the beam moment to be at 0.75 of its plastic moment. In specimen three it was considered irrational to calculate the displacement ductilities with respect to the beam plastic

moment when the connection was weaker than the beam. An arbitrary " μ " of 0.75 was assumed to occur when there was a load of 46 kN on the beam ends. This was about 20% less than that used in specimens one and two and about 30% less than the theoretical beam load to coincide with the strength of the calculated weakest part of the connection, i.e. the column flange in the beam tension flange region. The use of this load also led to similar beam end displacements between specimens three and specimens one and two for corresponding ductilities.

The loading sequence was the same for each of the specimens except for some variation in the final cycle of each test. The loading sequence for specimens one, two and three are shown in Fig's 5.1, 5.2 and 5.3 respectively.



(a) Building frame subjected to earthquake motions.



(b) Test beam-column assembly.

(c) Real beam-column situation.

FIG. 4.1 The specimen as part of a building.

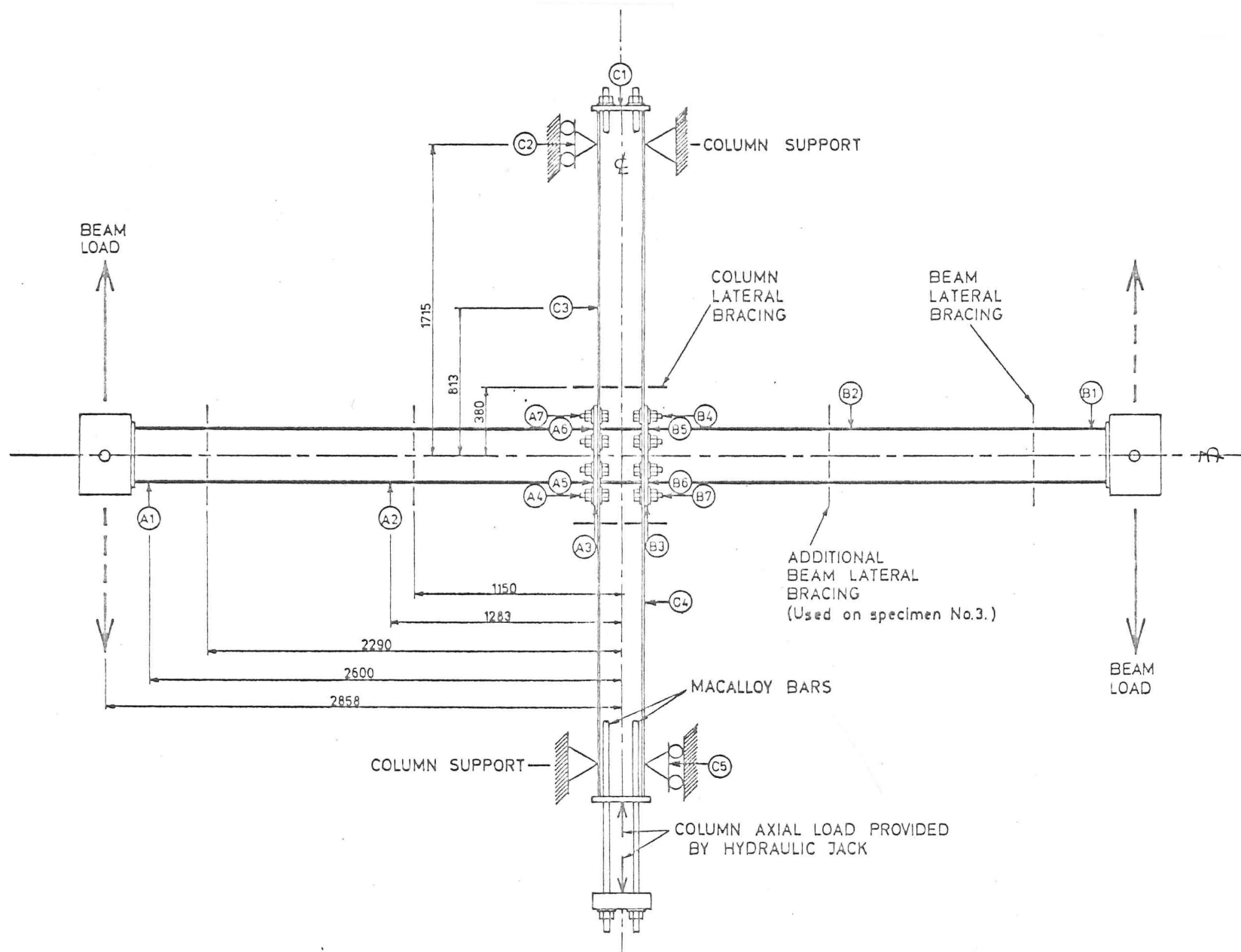


FIG. 4.2 Plan of the specimen, lateral bracing, dial gauges and load positions.

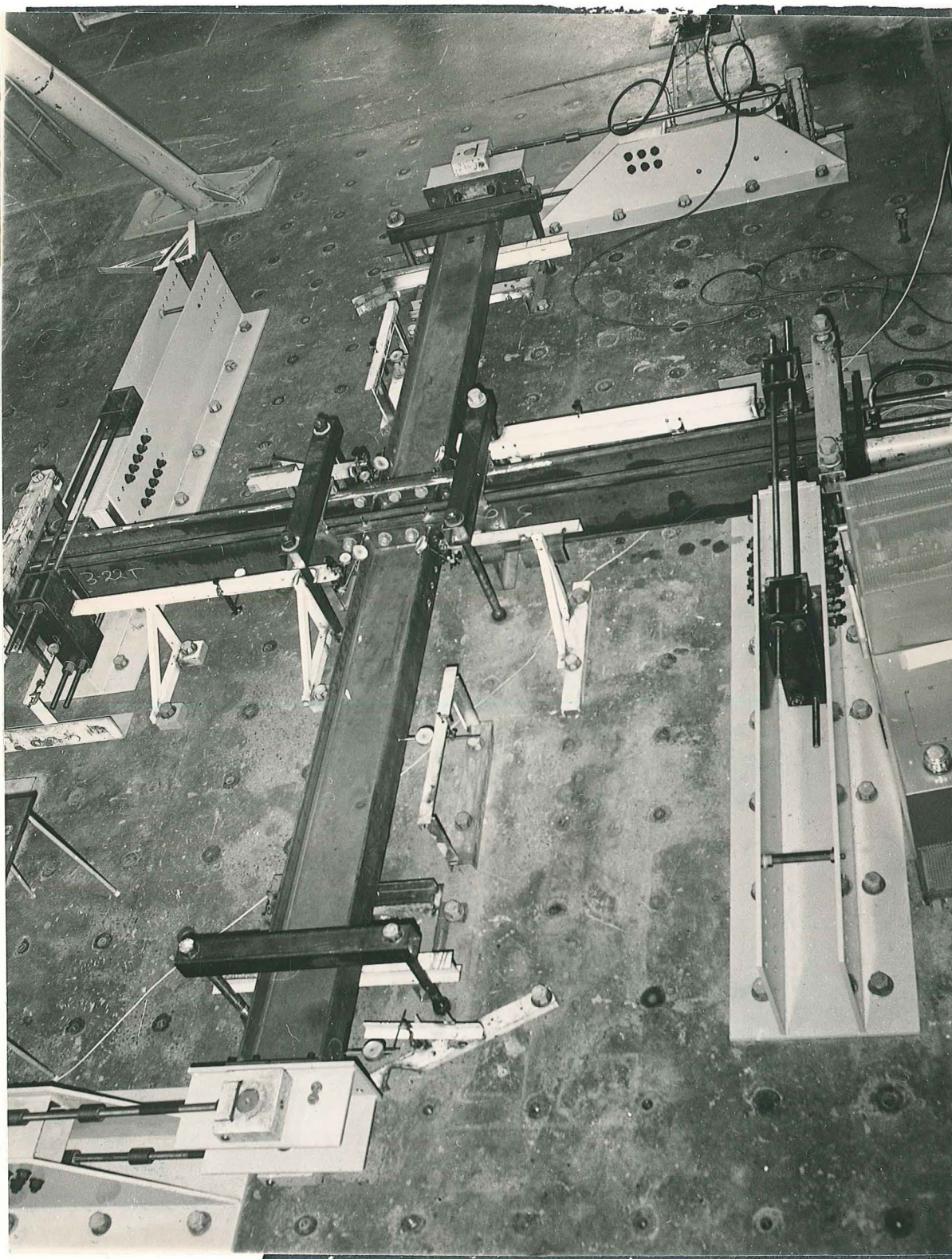
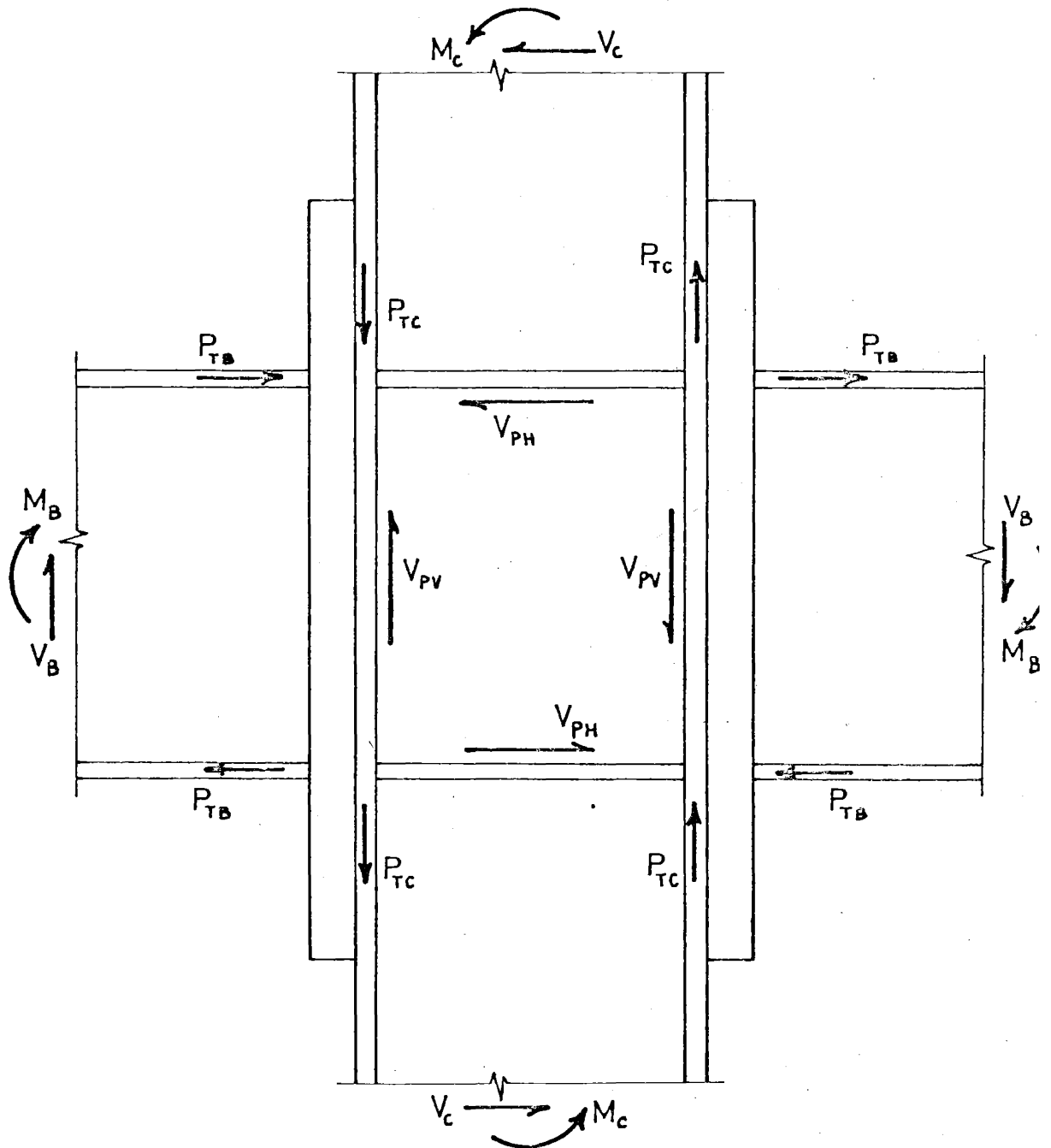


FIG. 4.3 Specimen one prior to testing.



$$V_{PV} = 2P_{TC} - V_B$$

$$V_{PH} = 2P_{TB} - V$$

FIG. 4.4 Shear forces in the panel zone.

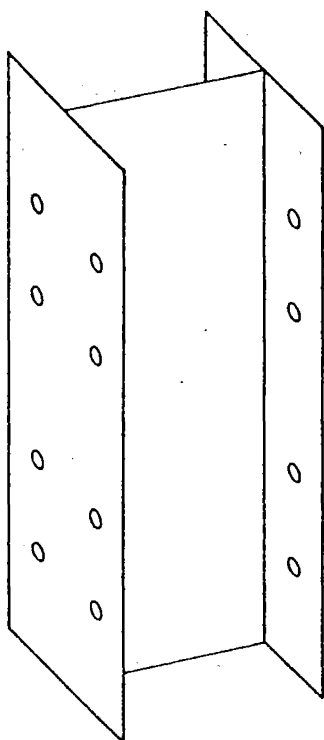


FIG. 4.5 Unstiffened column flanges.

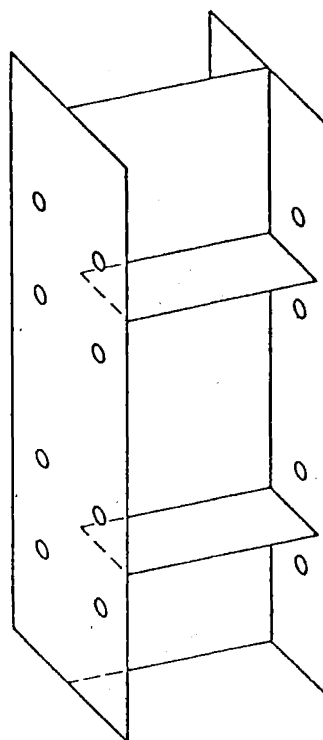


FIG. 4.6 Horizontal column flange stiffeners welded to the flanges and web.

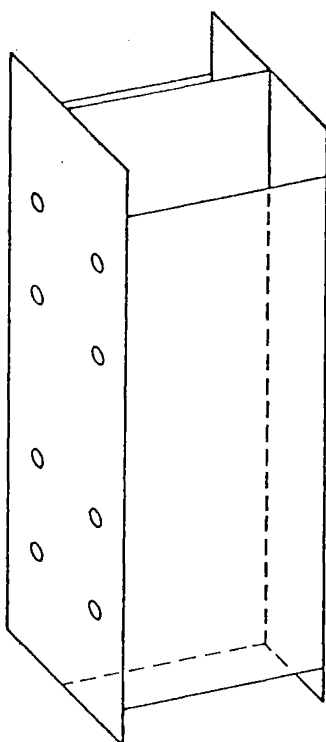


FIG. 4.7 Column flanges stiffened by the doubler plate welded to the column flange tips.

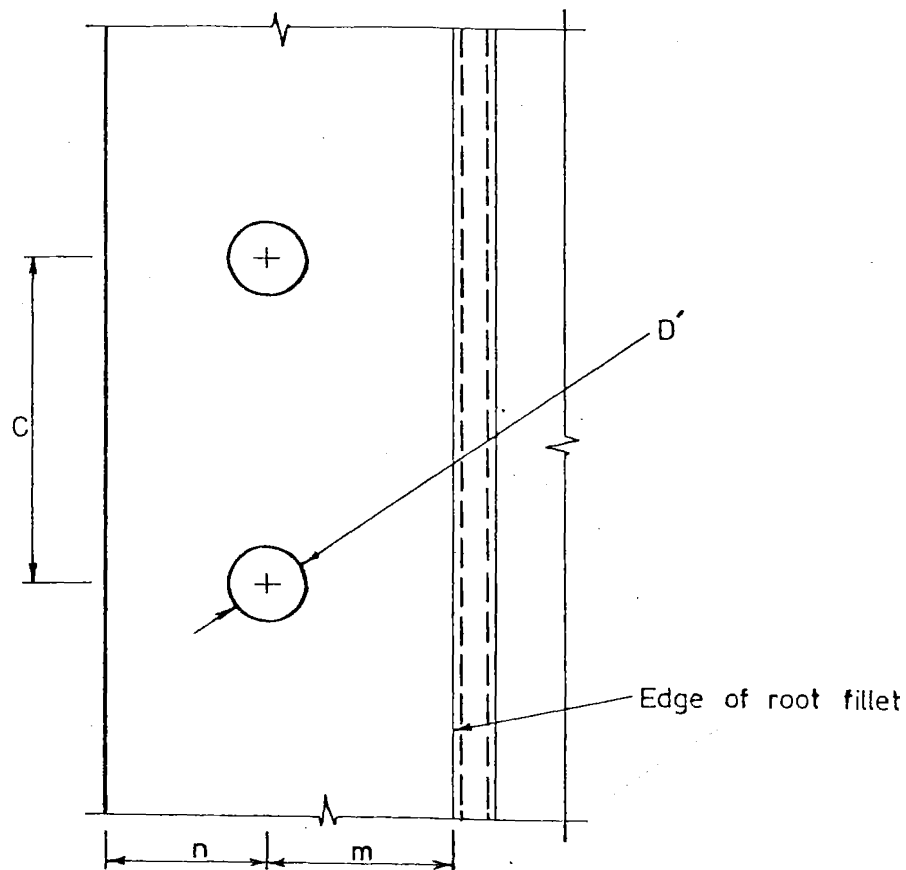


FIG. 4.8 Dimensions related to the unstiffened column flange capacity.

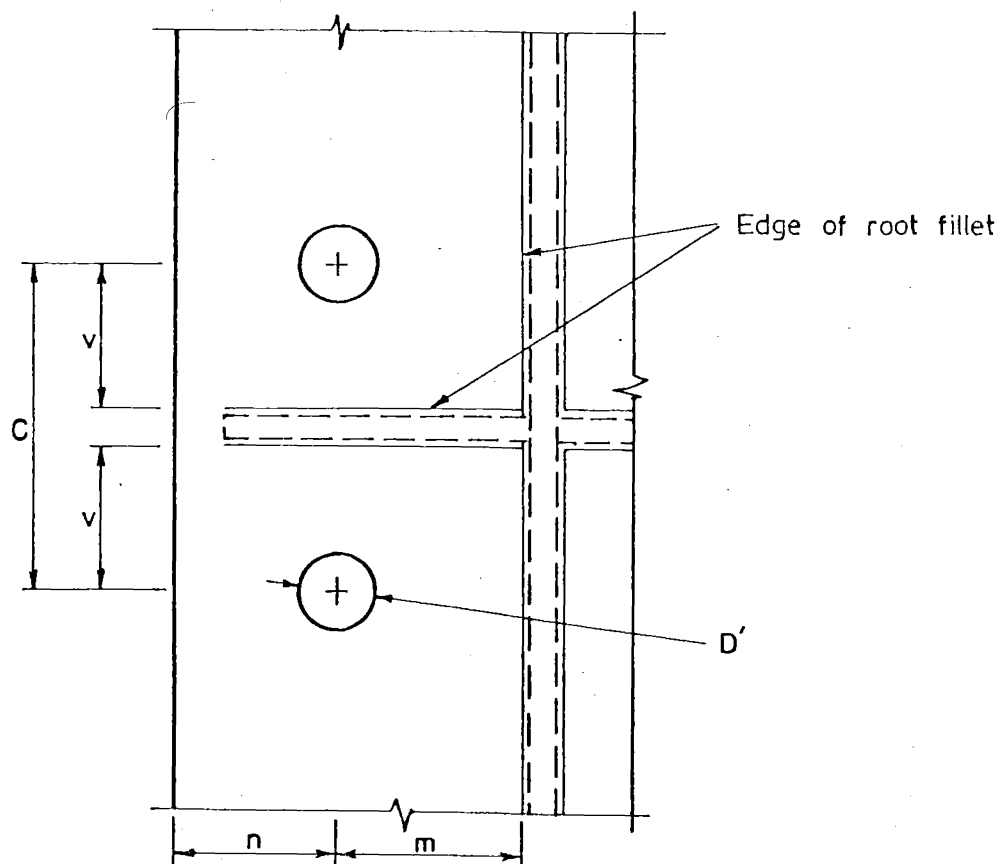


FIG. 4.9 Dimensions related to the column flange capacity when stiffened horizontally at the level of the beam flanges.

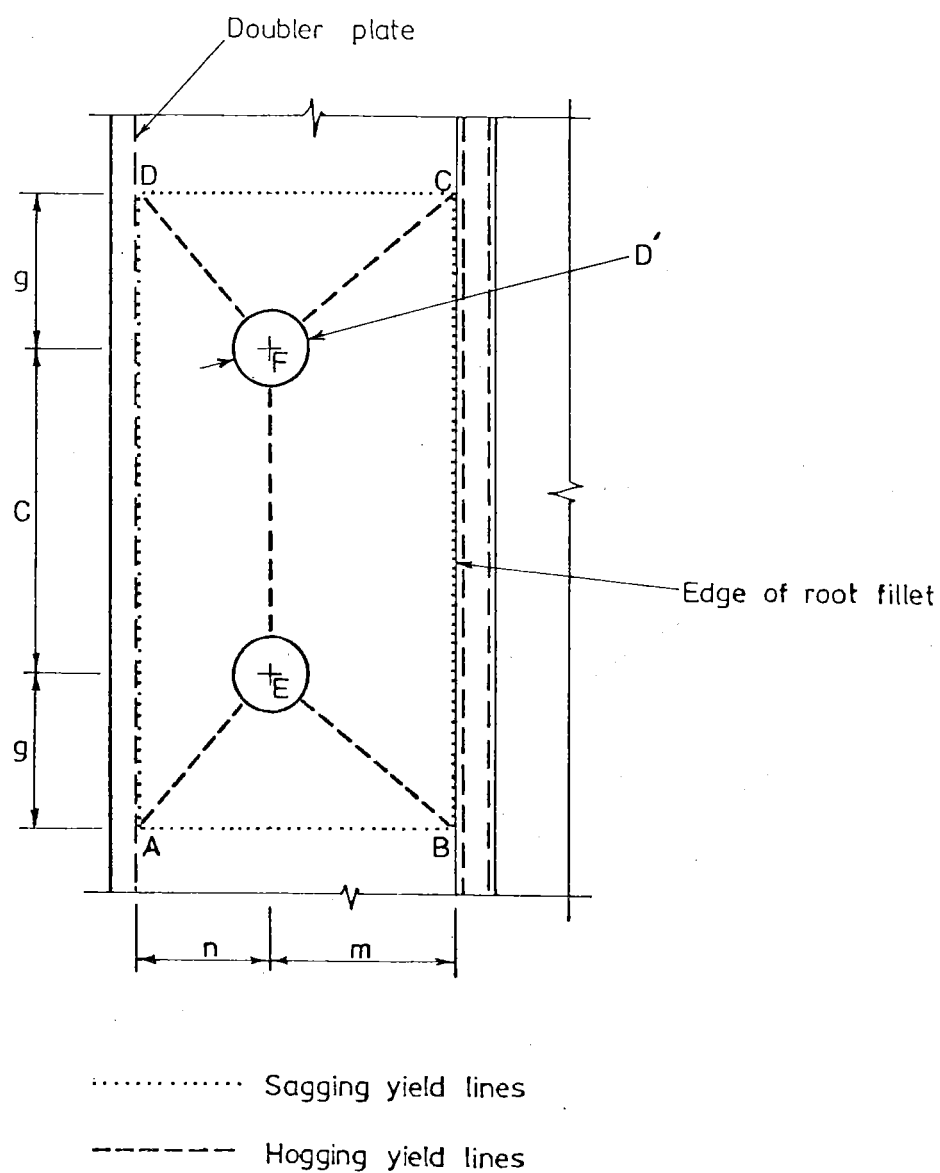


FIG. 4.10 Dimensions related to the column flange capacity when stiffened with doubler plates at the column flange tips.

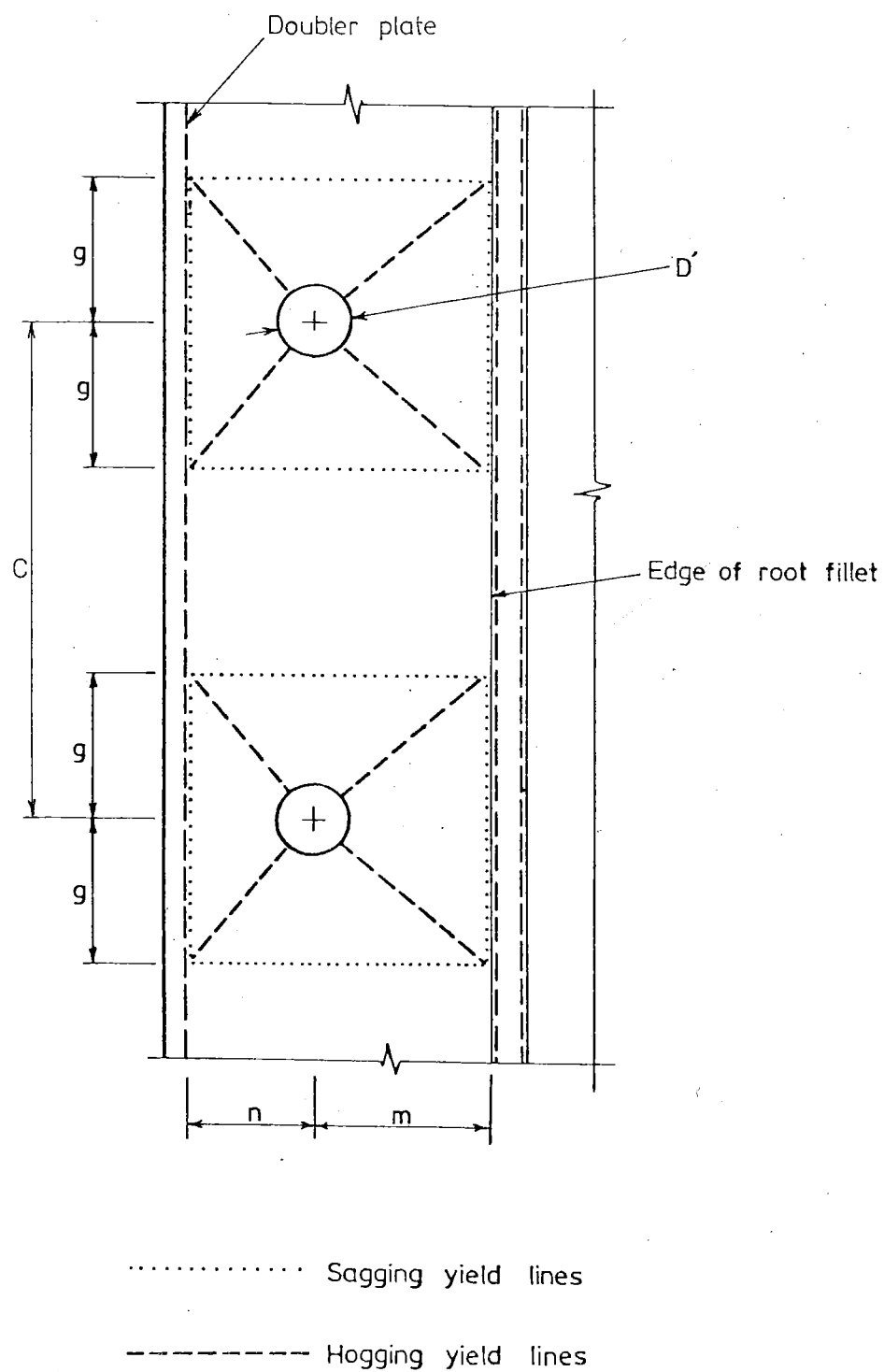


FIG. 4.11 Yield line pattern of Fig. 4.9 when "C" is large.

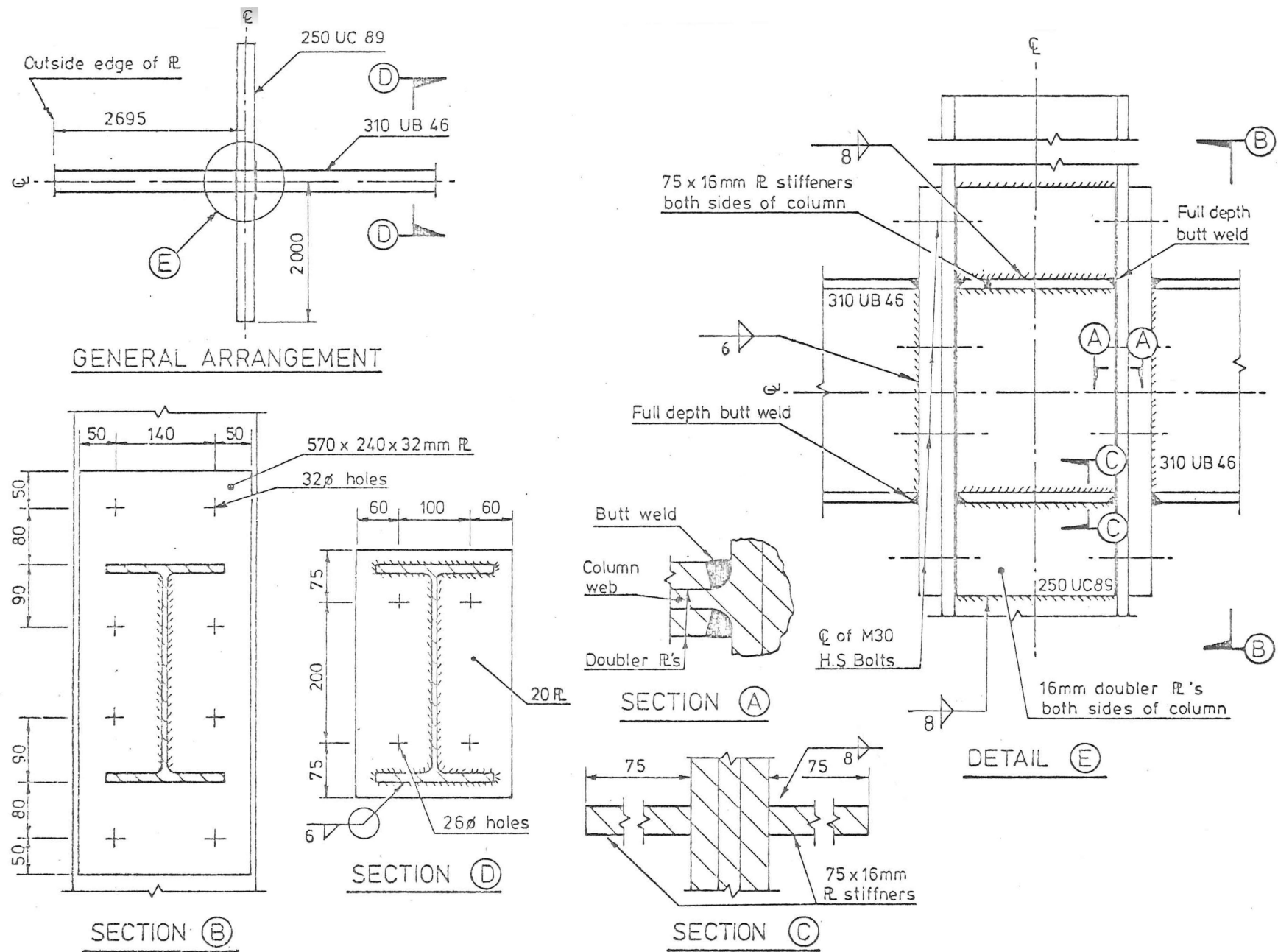
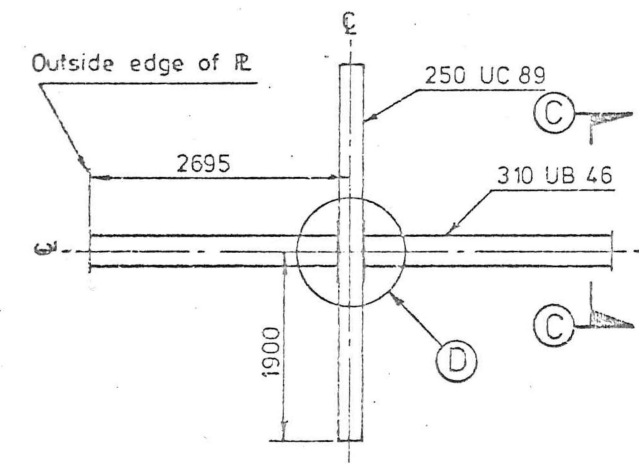
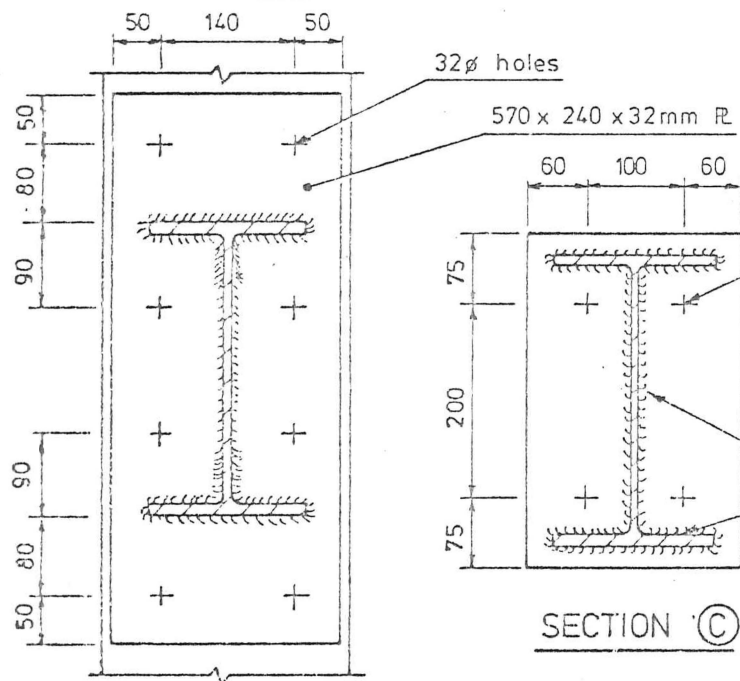


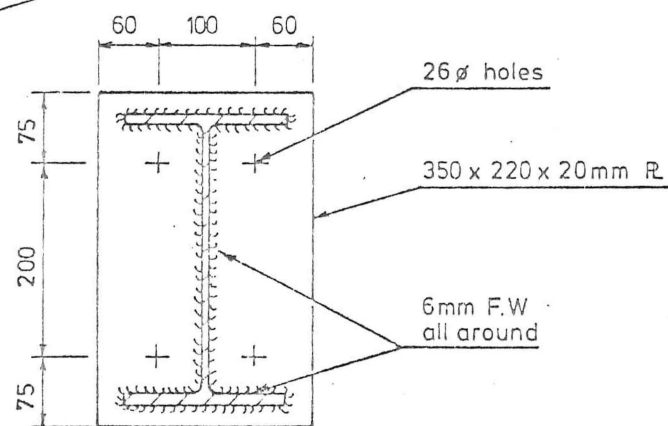
FIG. 4.12 Details of specimen one.



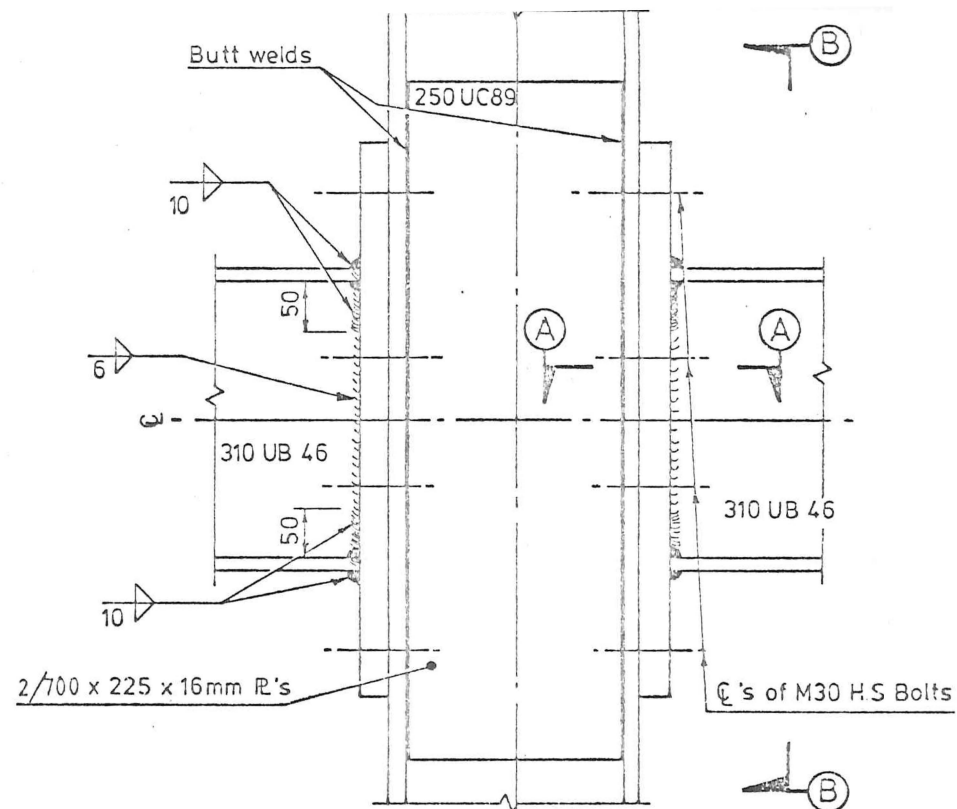
GENERAL ARRANGEMENT



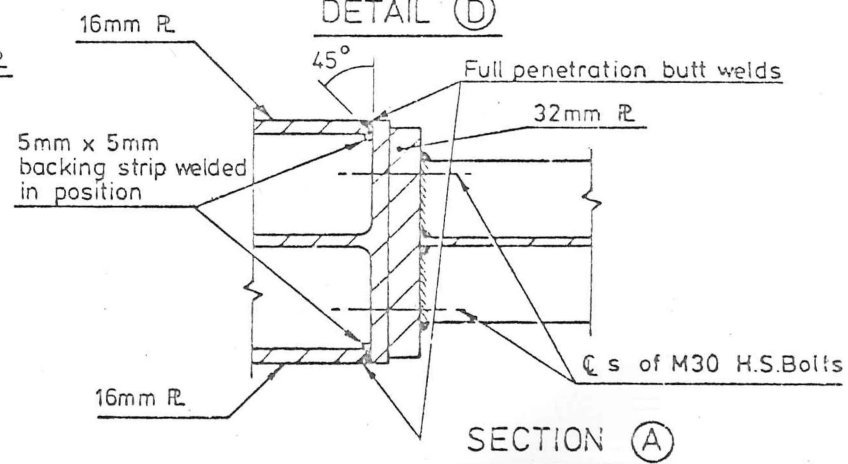
SECTION (B)



SECTION (C)



DETAIL (D)



SECTION (A)

FIG. 4.13 Details of specimen two.

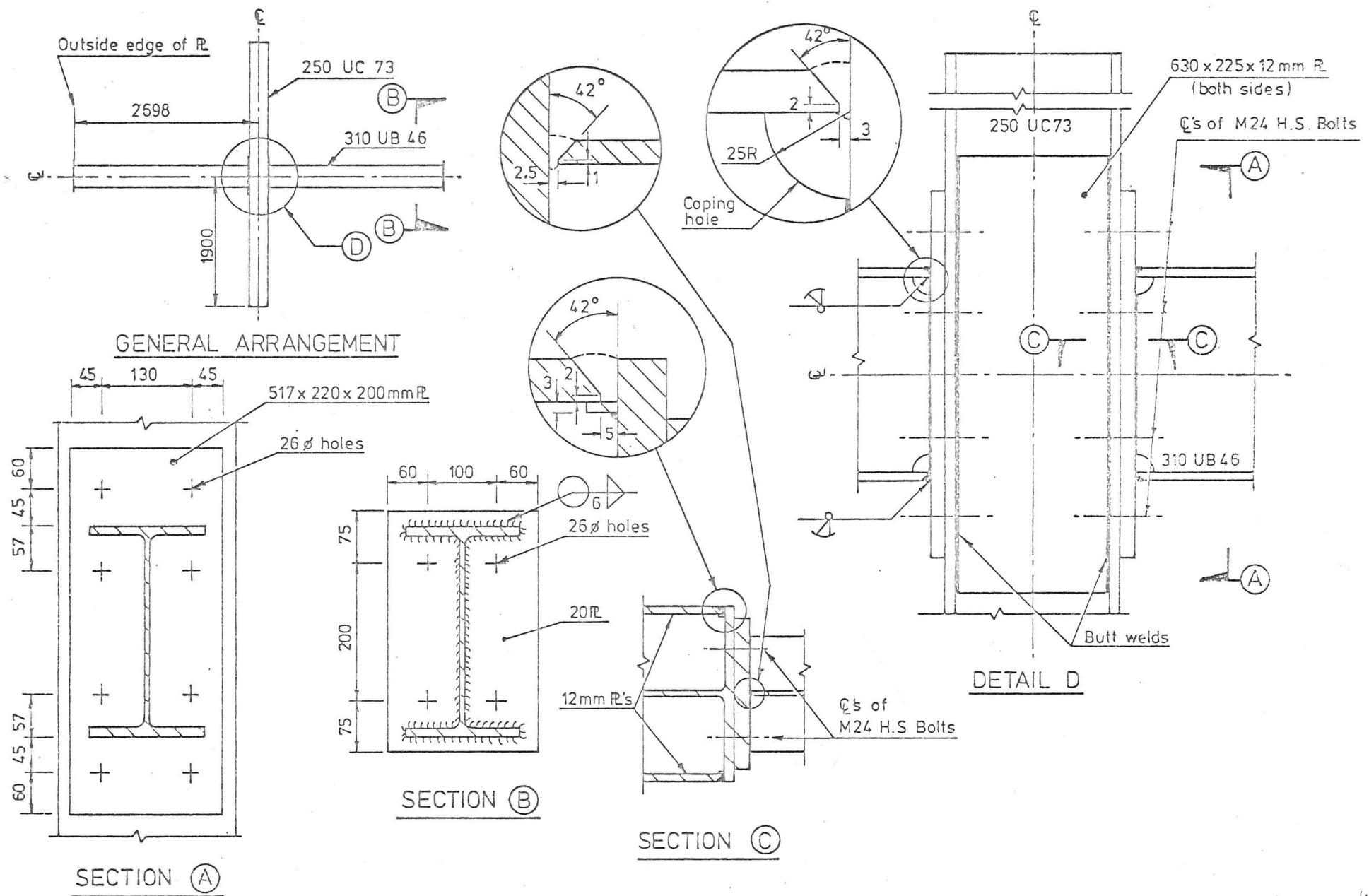


FIG. 4.14 Details of specimen three.

CHAPTER 5

RESULTS

5.1 SPECIMEN ONE

The loading sequence that was used is shown in Fig. 5.1.1 and the resulting beam load versus deflection records were plotted on Fig's 5.1.2 and 5.1.3 for beams "A" and "B" respectively. In the early stages of the test there were some indications of premature yielding in the panel zone and in the beam adjacent to the end plate. These were thought to be due to the existence of some residual stresses that resulted from the welding stage of the fabrication. Yielding occurred first in the beams and soon after in the panel zone, end plate and column flanges.

The main component of the displacements measured at the end of the beams (A1 and B1, see Fig. 4.2) was due to deformation within the beam itself. In the initial elastic stage of the loading the beam bending contributed a little over 50% towards the beam and deflections. Later on in the inelastic stages it was contributing over 90% of the beam end deflections. The remaining contributions being due to the deformation of the column in flexure and shear, the panel zone in shear, the column flanges around the tension bolts, the column web and stiffeners under the beam compression flange, the beam end plate, and the bolts. The beams started to bend and twist laterally out of the plane of loading after ductilities of $\mu = 4$ had been reached. This out of plane bending and twisting was partially restrained by the bracing. The load carrying capacity of the specimen continued to rise until maximum loads were reached at approximately $\mu = 5$. The maximum loads for beams "A" and "B" were respectively 106 kN and 104 kN. After this beam flange buckling occurred and the load carrying capacity of the specimen slowly dropped off. The beam flange buckle was located near the end plate in the beam compression flange and on the side of the beam that had additional compressive stresses due to the out of plane deformation of the beams. Refer to Fig's (5.1.4(a) and (b)).

Yielding in the end plate was most obvious along the general line of the beam tension flange although it was also evident in the region between the beam flanges. The end plate outside the beam tension flange did not appear to act in double curvature as had been assumed in its design. However, deformations in the end plates were relatively small and can be seen in Fig's 5.1.5 and 5.1.6.

Some yielding occurred in the column flanges around the beam tension flange bolts. The resulting deformations were slightly less than those in the end plate. During the fabrication of specimen one the horizontal column flange stiffeners pulled the column flanges inwards. This made visual assessment of the column flange deformations deceptive and so with respect to Fig's 5.1.5 and 5.1.6 one should only compare the column flange deformations in the beam tension flange region with reference to those in the beam compression flange region.

Shear deformations in the panel zone did not contribute much to the deflections at the beam ends. However, measurement of strains in the panel zone indicated that yielding was occurring. When the specimen was at a displacement ductility factor, " μ ", of 6 the strains in the panel zone exceeded yield in shear by a factor of about 2.

Elongation and bending of the bolts was very minimal in this specimen. Some yielding occurred in the column on either side of the connection due to axial load and flexure but this yielding was not very significant. A general view of the specimen after testing is shown in Fig. 5.1.7.

5.2 SPECIMEN TWO

The loading sequence that was followed is shown in Fig. 5.2.1 and the resulting beam versus deflection records were plotted on Fig's 5.2.2 and 5.2.3 for beams "A" and "B" respectively. There were again some signs of premature yielding in the beam and panel zone doubler plates although relative to specimen one these were not quite as significant in the doubler plates. Generally yielding occurred first in the beams and then in the panel zone, end plates and column flanges.

The beams in this specimen behaved in very much the same way as those in specimen one. After extensive yielding had occurred from in plane bending the strength of the beams became ultimately governed by lateral instability and beam flange buckling as shown in Fig's 5.2.4 and 5.2.6. The maximum load on beam "A" was 114 kN at $\mu = 5.5$ and on beam "B" was 106 kN at $\mu = 6.0$. It is suspected however that some friction was introduced between beam "A" and the lateral bracing in the last cycle of this test because of the large amount of beam twisting.

Yielding in the end plates occurred mainly in the region of the beam flanges, as shown in Fig. 5.2.5. This was the case in specimen one although relative to specimen one the end plate deformations were less. Compare Fig's 5.1.6 and 5.2.5. Yielding occurred in the column flanges around the beam tension flange bolts. The magnitude of these deformations was similar to those in specimen one.

Shear deformations in the panel zone were again not visually obvious but measurements taken indicated significant yielding. When the specimen was at a displacement ductility, " μ ", of 6 the strains in the panel zone had exceeded yield in shear by a factor of about 1.5.

Elongation and bending of bolts was again very minimal. Some yielding occurred in the column on either side of the connection but was relatively insignificant. A general view of the specimen after testing is shown in Fig. 5.2.6.

5.3 SPECIMEN THREE

The loading sequence that was followed is shown in Fig. 5.3.1 and the resulting beam versus deflection records were plotted on Fig's 5.3.2 and 5.3.3 for beams "A" and "B" respectively. As in specimens one and two there were signs of premature yielding in the panel zone doubler plates and in the beams adjacent to the end plates.

The main single contributor to the beam end displacements was the beam deformations. In the initial elastic stage of the loading the beam bending contributed approximately 40% towards the beam end deflections. In the later stages of the test the beam bending continued to only provide about 40% of the beam end deflections.

Out of plane bending in the beams and beam flange buckling were not nearly as significant in this test. This is because the beam loads were lower and probably of more importance was that the beams had more lateral bracing as shown in Fig's 4.2 and 5.3.14. In the initial elastic stage of the test this specimen was 25% more flexible than specimens one and two.

The combined deformation of the end plate and column flange was approximately 3 times greater than that of specimen one and 4.5 times greater than that of specimen two for the same beam end displacement. The deflections in the beam "A" end plate were slightly larger than those in the beam "B" end plate. The beam "B" end plate was the one joined to its beam with the more largely splayed butt welds as mentioned before. After $\mu = 3$ in the $\mu = 6$ cycle signs of high stress could be seen in the end plate immediately adjacent to the tension flange butt weld. These were predominantly on the end plate outstand side of the beam tension flange weld. At $\mu = 4$ in the $\mu = 6$ cycle a cleavage fracture started to propagate through the end plate of beam "B". A view of this fracture after the completion of testing is shown in Fig's 5.3.8, 5.3.9 and 5.3.10. A close examination of the fracture revealed that there were no signs of lamellar tearing. The effect of this fracture on the specimen's capacity to resist the beam "B" load was indicated by the sudden drop in the load versus deflection relationship, Fig. 5.3.3. The deformation of an end plate when $\mu = +6$ is shown in Fig. 5.3.4 for comparison with that of specimen one, Fig. 5.1.6 and specimen two, Fig. 5.2.5.

The column flanges deformed around the four beam tension flange bolts as shown in Fig. 5.3.11. After fracture had occurred in the end plate of beam "B" the deformations in the beam "B" side column flange were predominantly around the two bolts that were taking most of the beam tension flange load, i.e. the two bolts immediately inside the beam tension flange. The resulting column flange deformations are shown in Fig. 5.3.12.

Measurements of strain in the panel zone showed that the yield strain in shear had been exceeded by a factor of about 4 when the test on the specimen was at $\mu = 6$. At a later stage in the test two fractures occurred between the doubler plate butt welds and the column flange tips. Both of these fractures were on the beam "B" side of the column. They were thought to have been initiated by the higher load demand in the two bolts immediately within the beam tension flange after the beam "B" end plate had fractured.

Fig's 5.3.8 and 5.3.12 show one of the fractures soon after it had started. Fig. 5.3.13 shows the fracture, on the other side of the column, when it had extended the full length of the doubler plate. These fractures occurred in the column flange material immediately next to the butt weld. Indications of some possible lamellar tearing action were evident in the fracture.

The maximum loads recorded on the beams were 102 kN, at $\mu = 10$, on beam "A" and 89 kN, at $\mu = 4$, on beam "B". Some of the bolts showed signs of deformation especially in bending. This was largely due to the relative movement of the column flanges and end plates from their initially parallel orientation.

Some signs of yielding in the column outside of the connection were evident, especially in the column flanges and web immediately outside the stabilising influence of the doubler plates. This can be seen in the left and right hand sides of Fig. 5.3.13 by the cracking and flaking of the white plaster.

One feature that was common to all the specimens was that throughout the cyclic loading procedure of the tests the columns were progressively shortened. This was most significant in the column connection region but was also evident in the adjacent column section. General views of the specimen during the test are given in Fig's 5.3.5, 5.3.6 and 5.3.7.

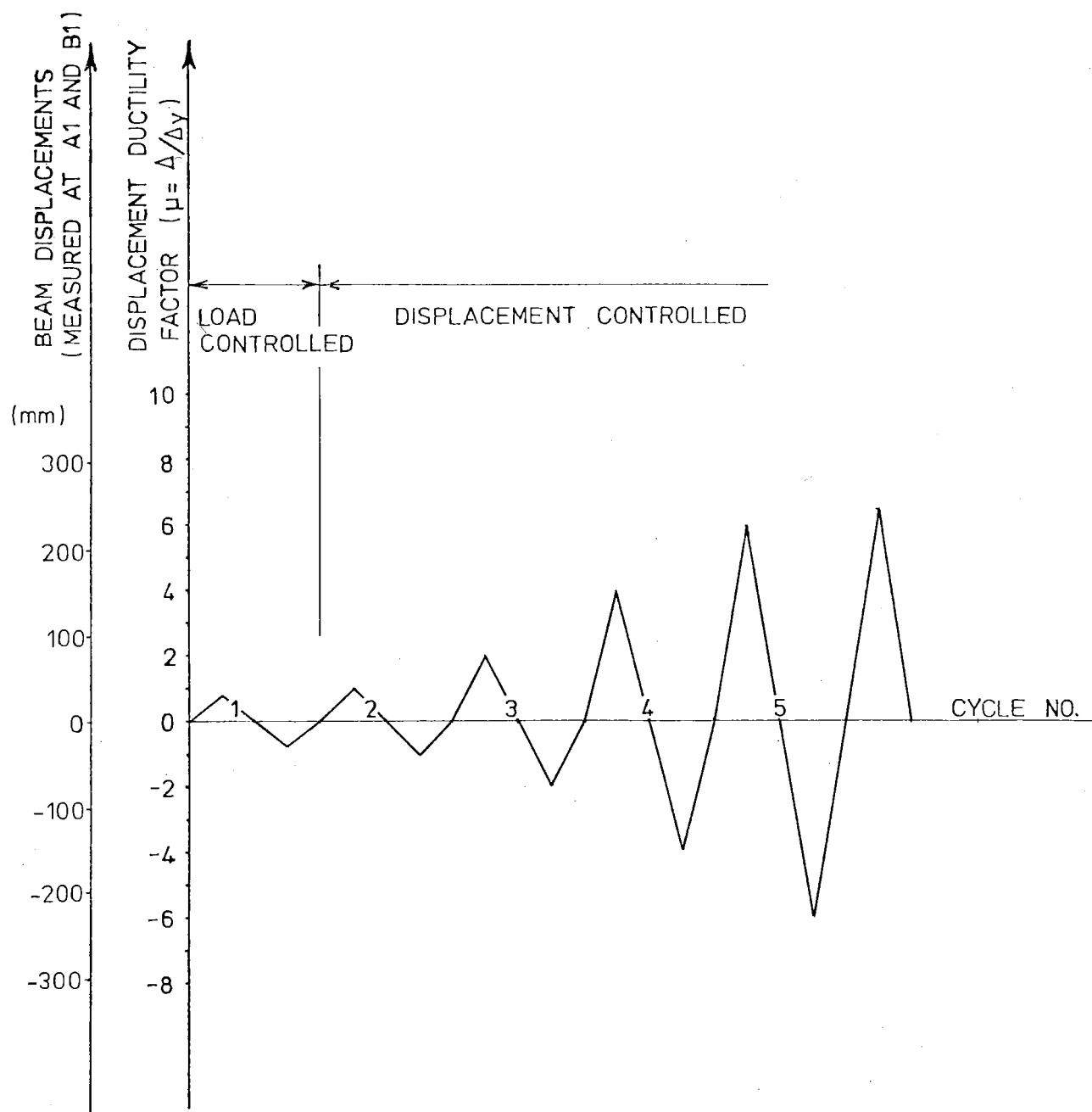


FIG. 5.1.1 Loading pattern, specimen one.

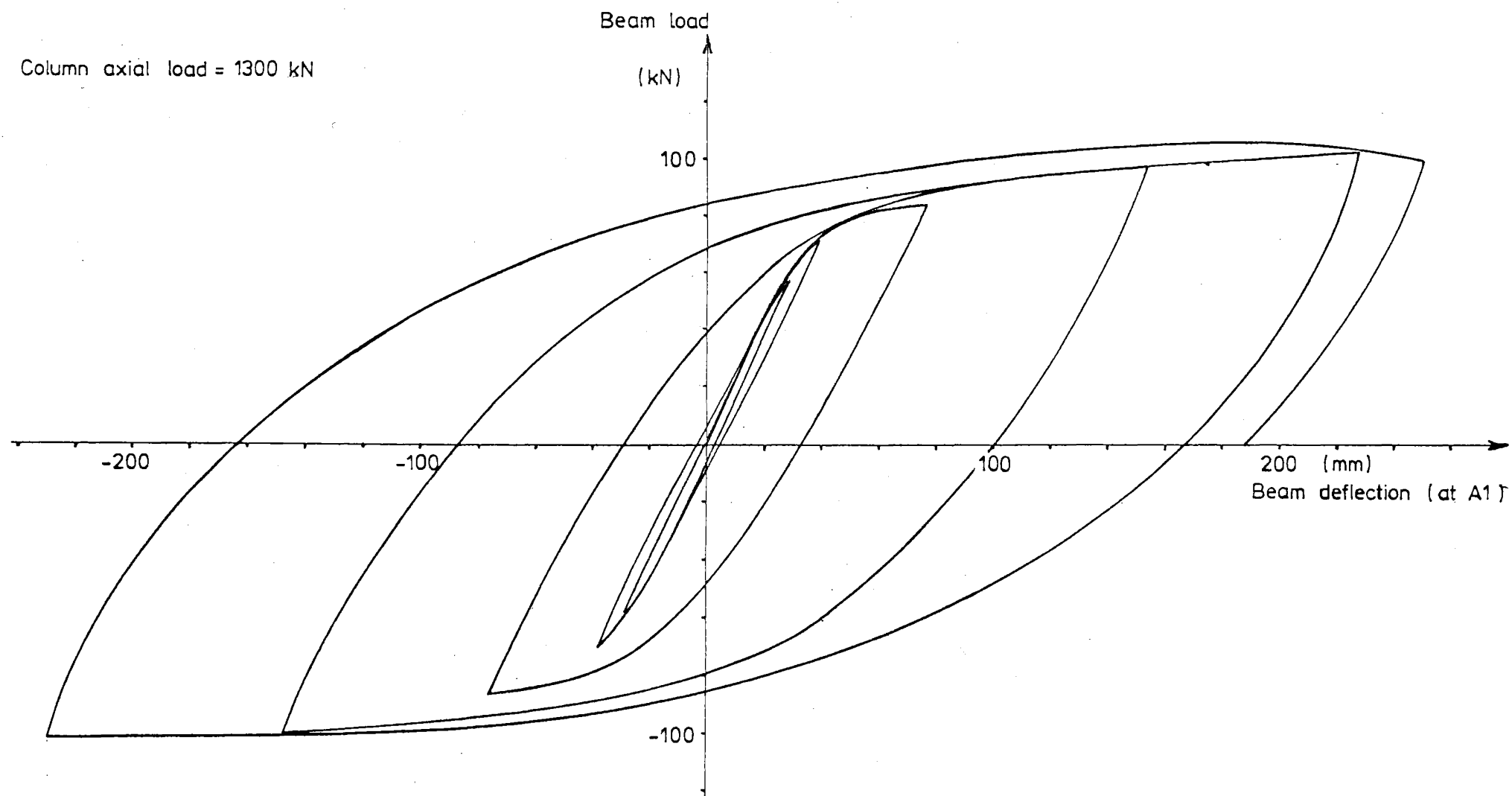


FIG. 5.1.2 Load versus deflection, beam "A", specimen one.

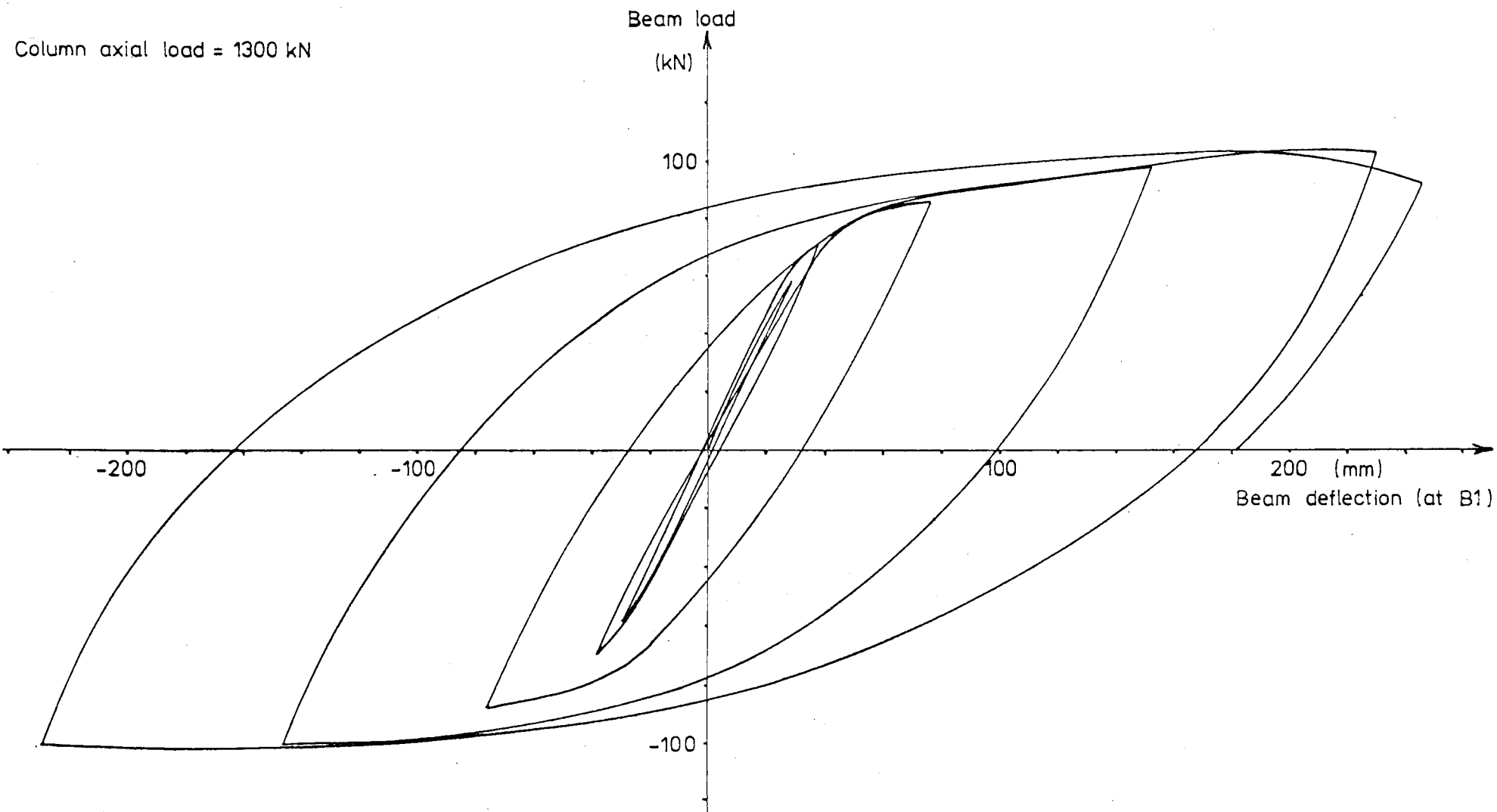
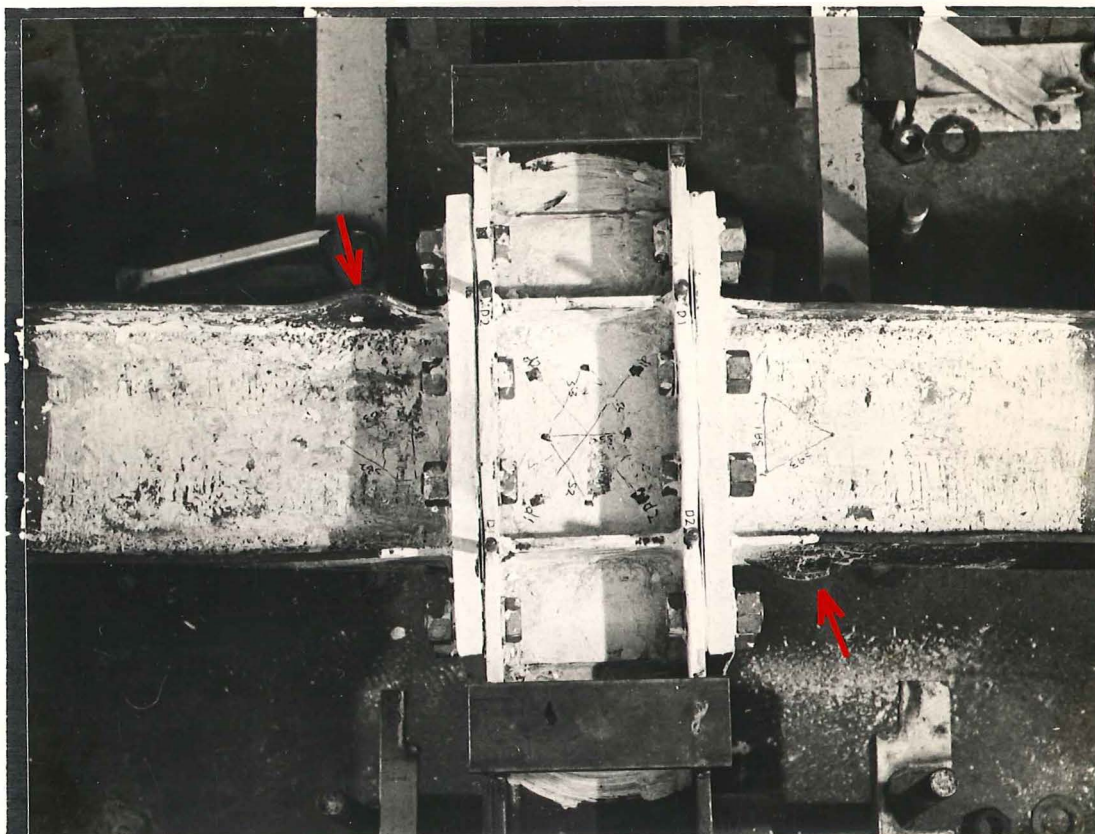
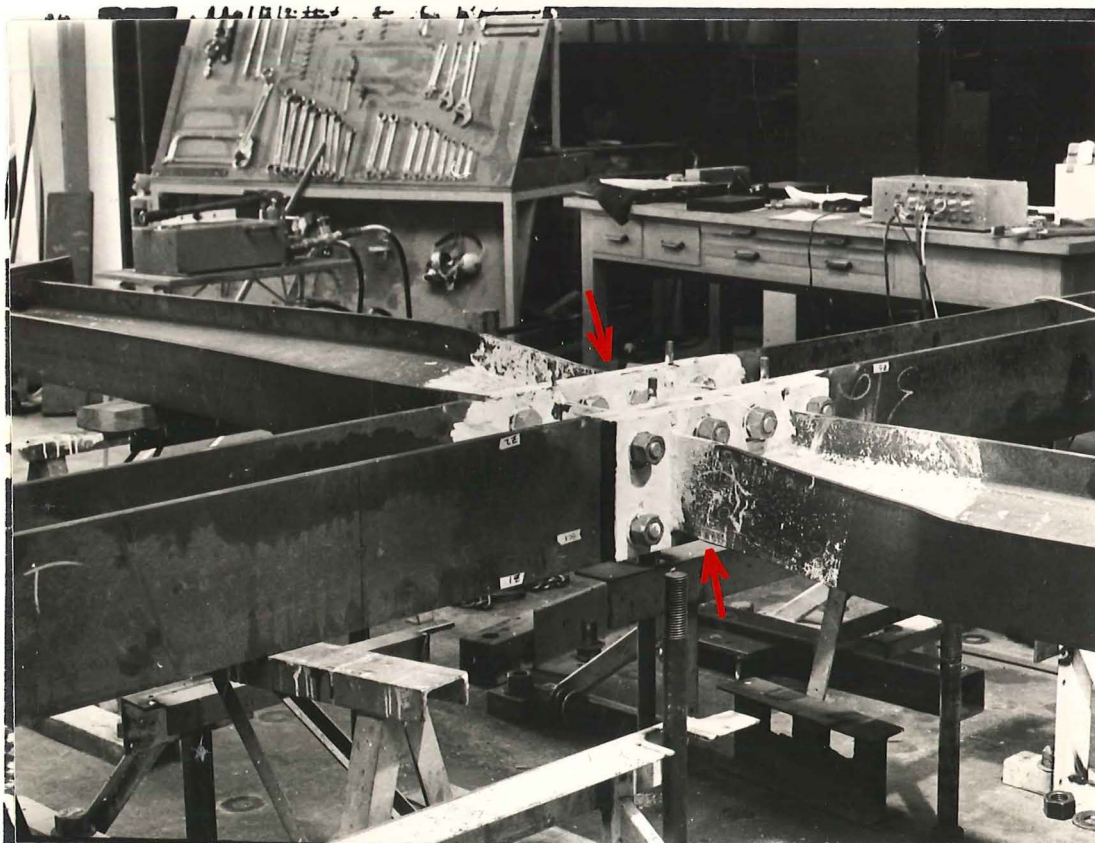


FIG. 5.1.3 Load versus deflection, beam "B", specimen one.



(a) Close up view of the connection.



(b) General view of the specimen.

FIG. 5.1.4(a) and (b) Buckling of the beam flanges, (specimen one).

The locations of the buckles are indicated on the photographs.

(Beam "B" on left and Beam "A" on right).

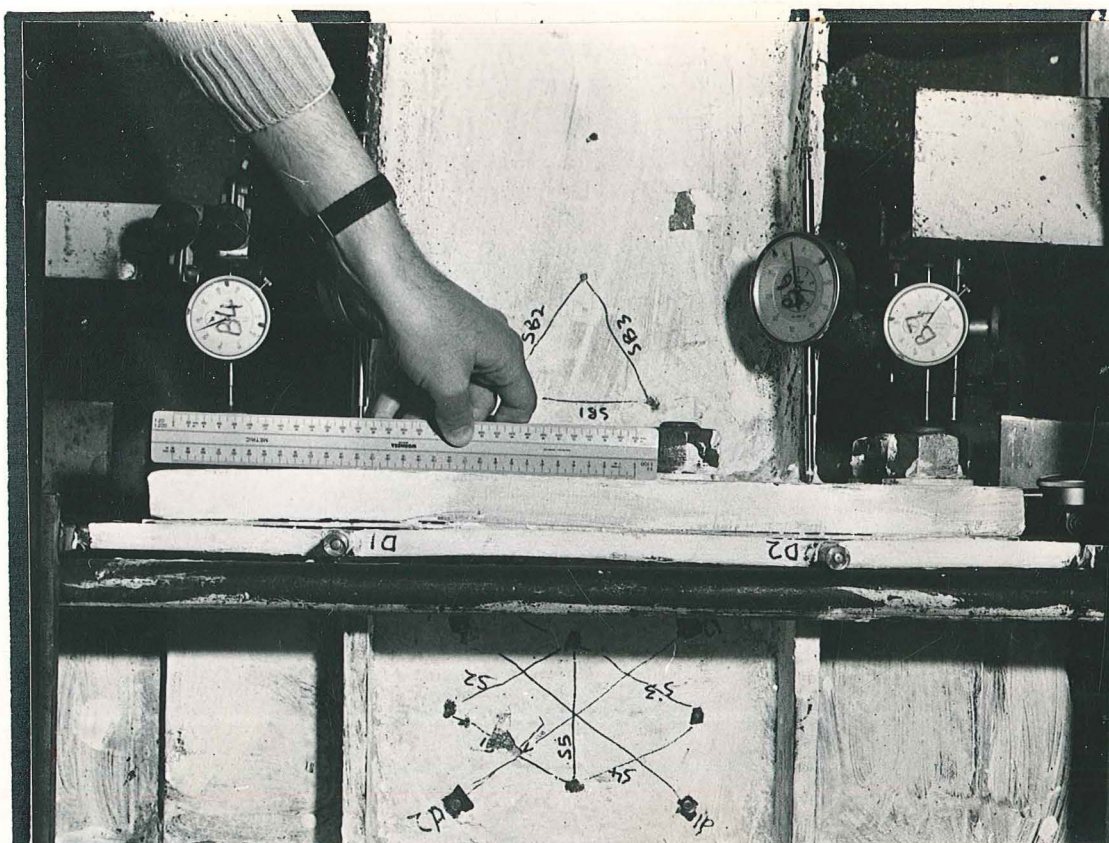


FIG. 5.1.5 End plate of beam "B", specimen one, when $\mu = +4$, in the $\mu = 4$ cycle.

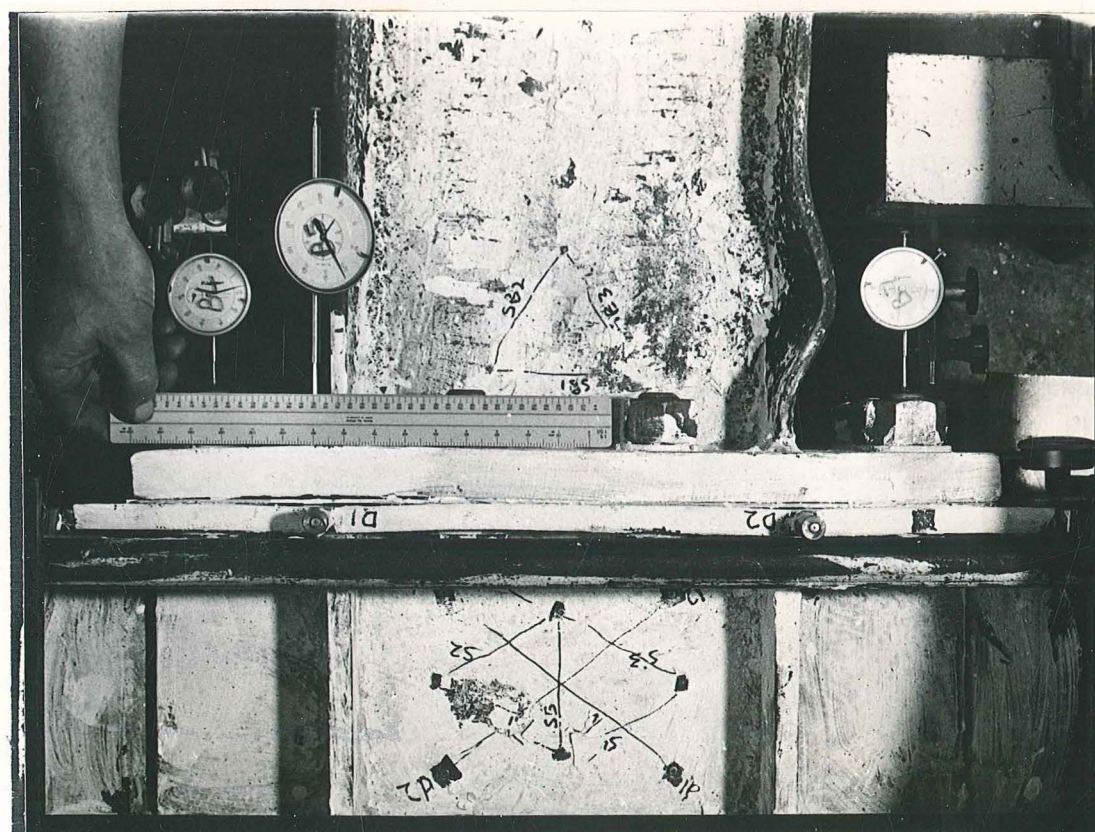


FIG. 5.1.6 End plate of beam "B", specimen one, when $\mu = + 6.6$.

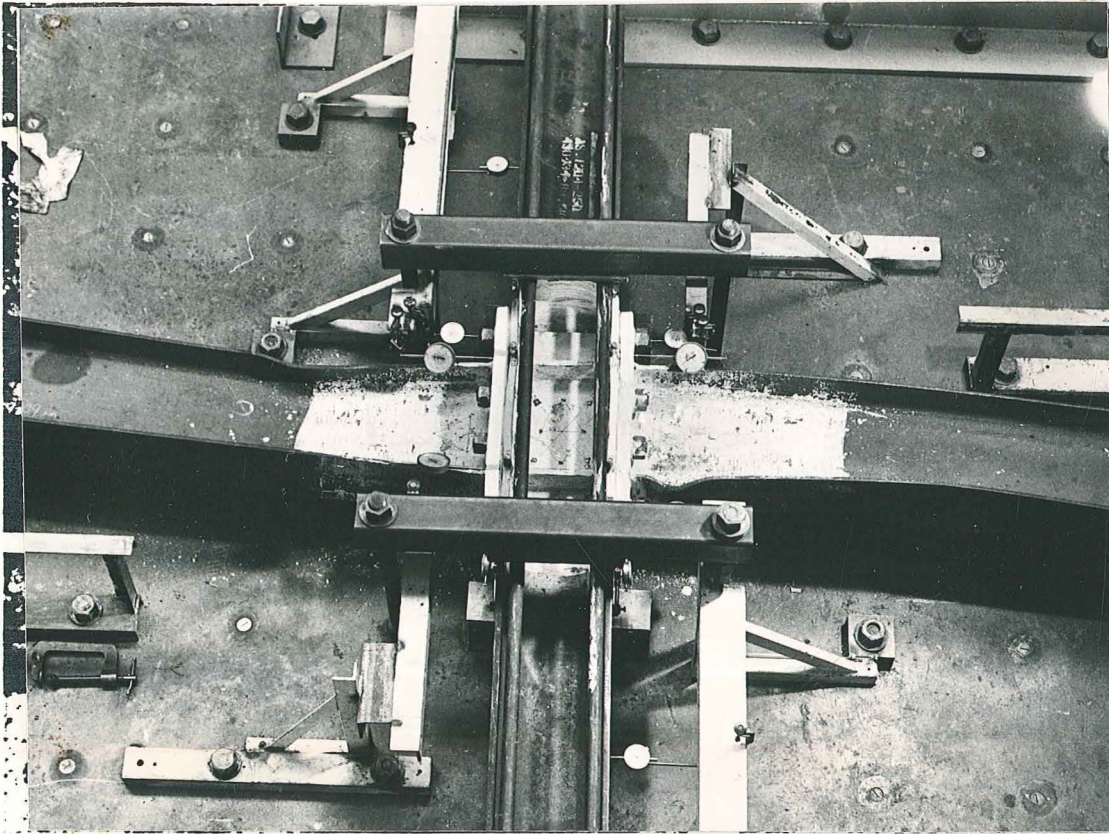


FIG. 5.1.7 Specimen one after testing.
Beam "A" on left, Beam "B" on right.

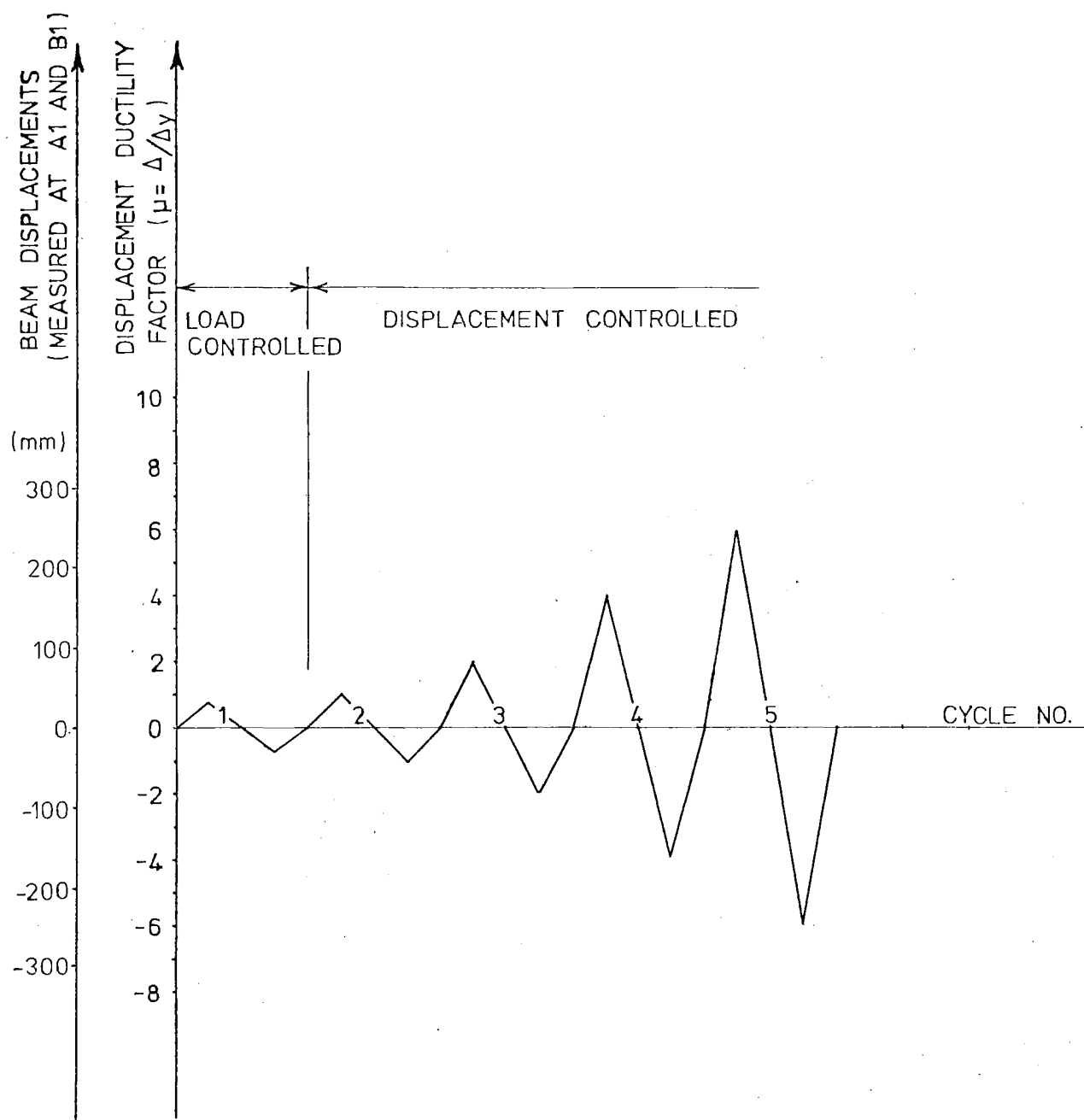


FIG. 5.2.1 Loading pattern, specimen two.

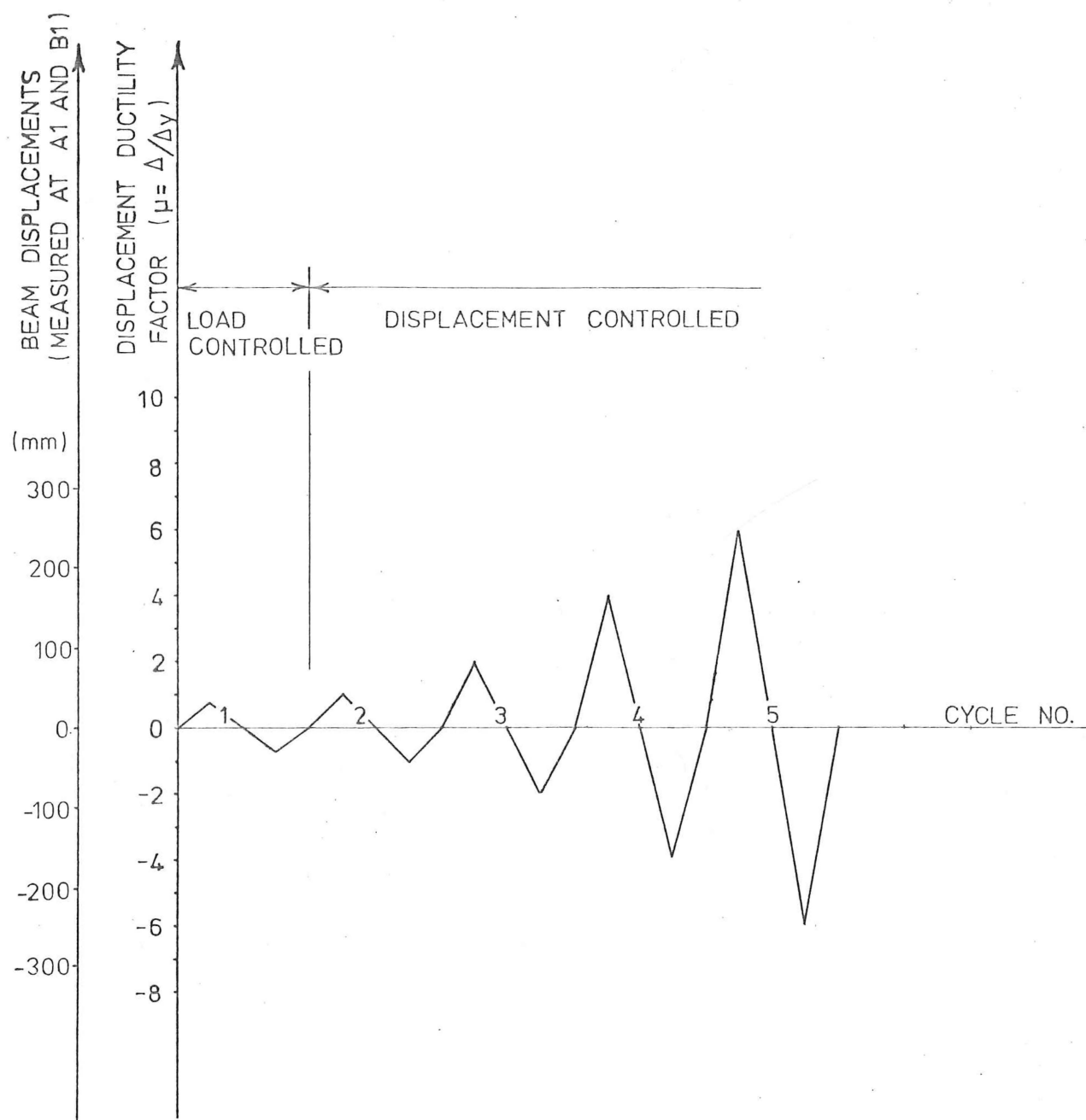


FIG. 5.2.1 Loading pattern, specimen two.

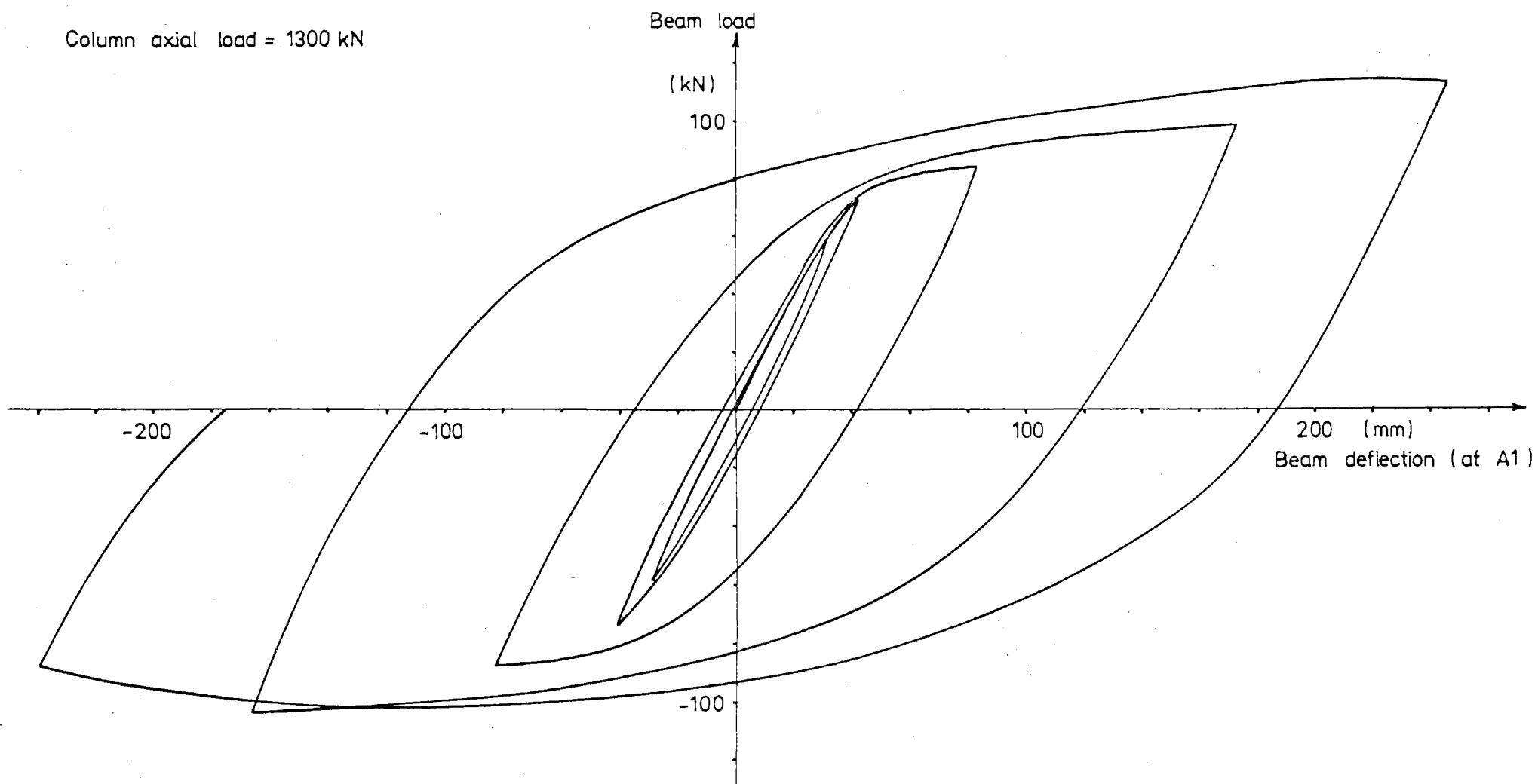


FIG. 5.2.2 Load versus deflection, beam "A", specimen two.

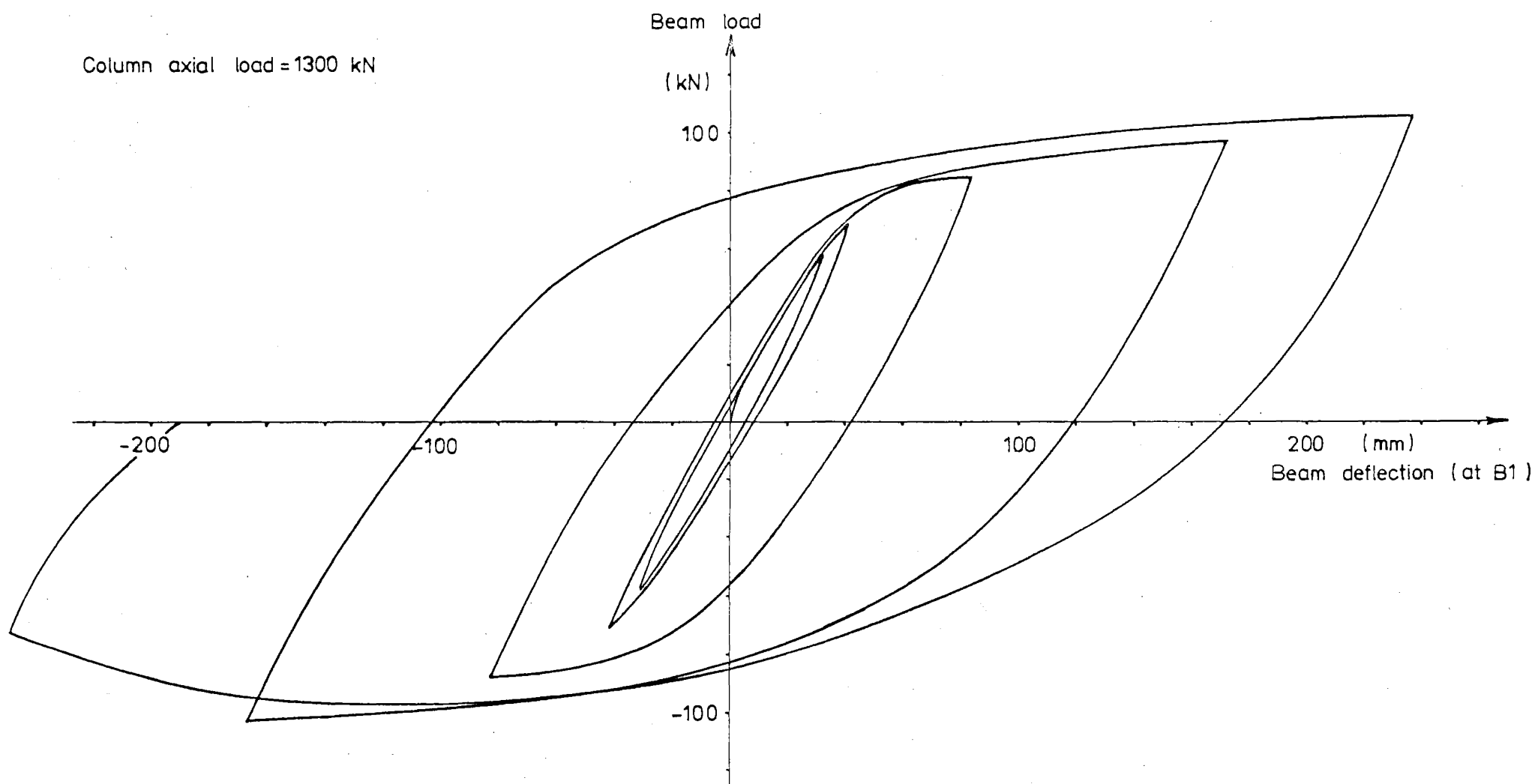


FIG. 5.2.3 Load versus deflection, beam "B", specimen two.

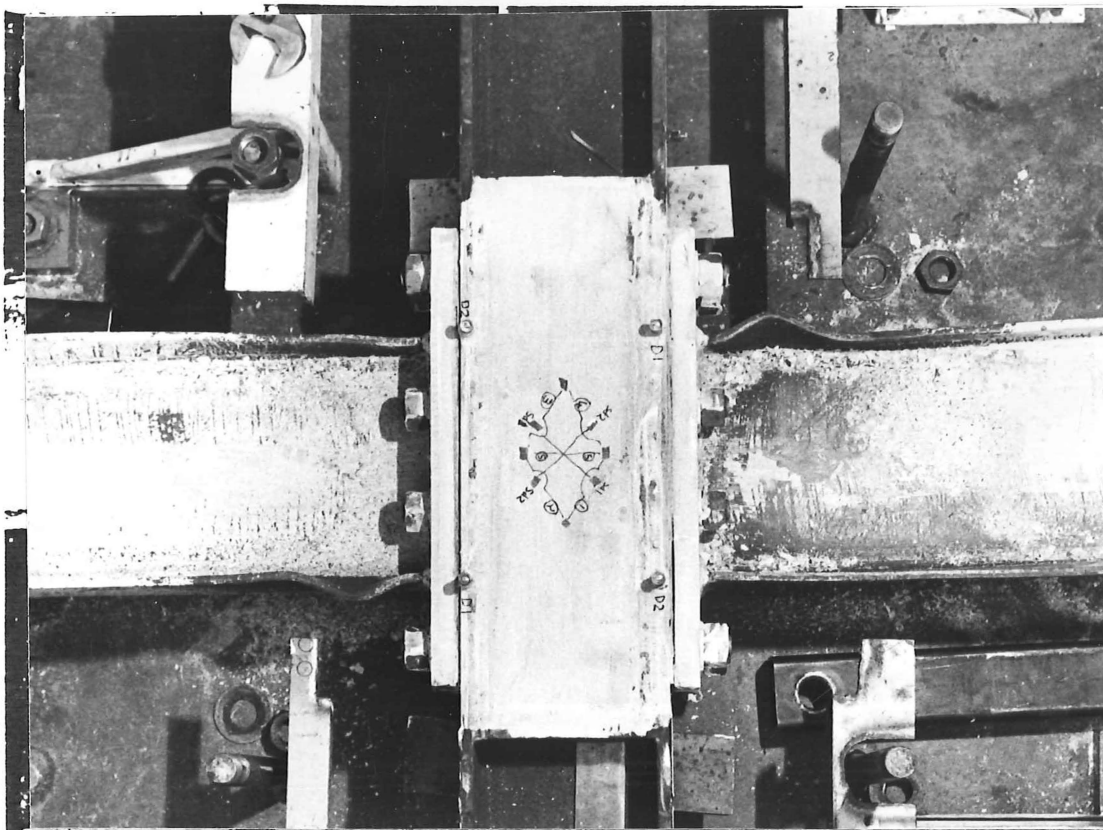


FIG. 5.2.4 Buckling of the beam flanges,
specimen two, after test.

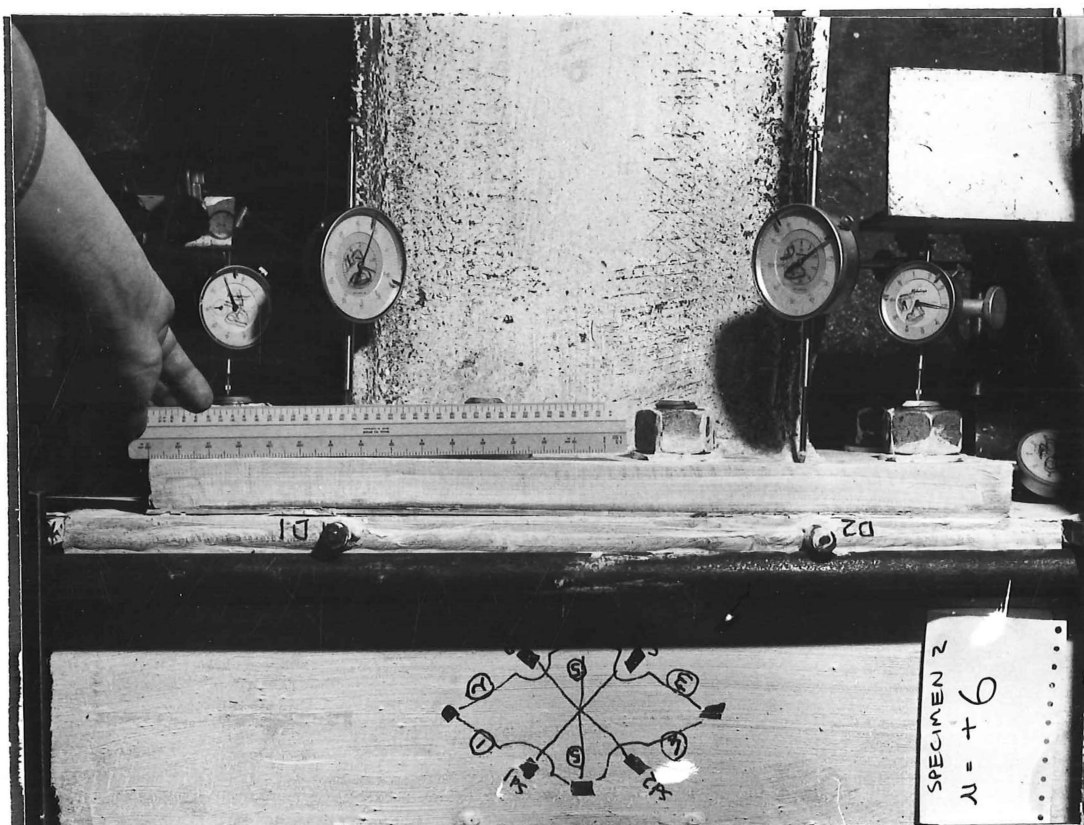


FIG. 5.2.5 End plate of beam "B", specimen two,
when $\mu = + 6$.

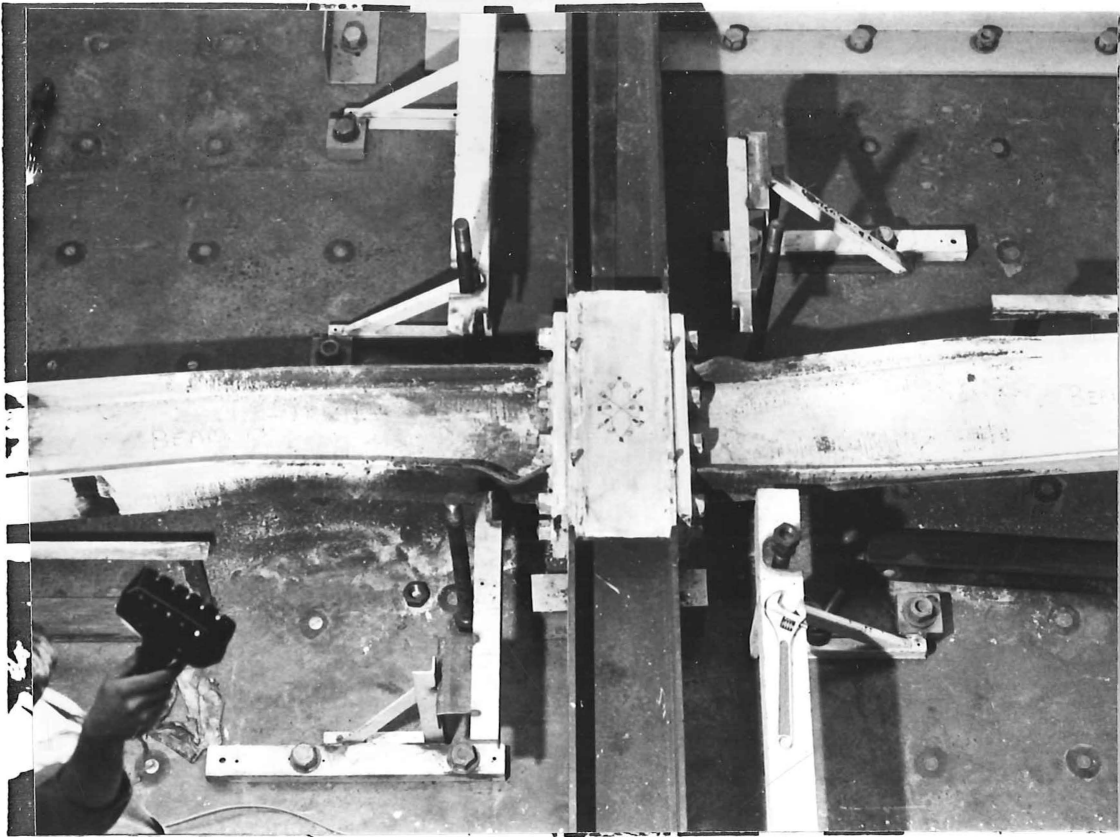


FIG. 5.2.6 General view of specimen two after test.

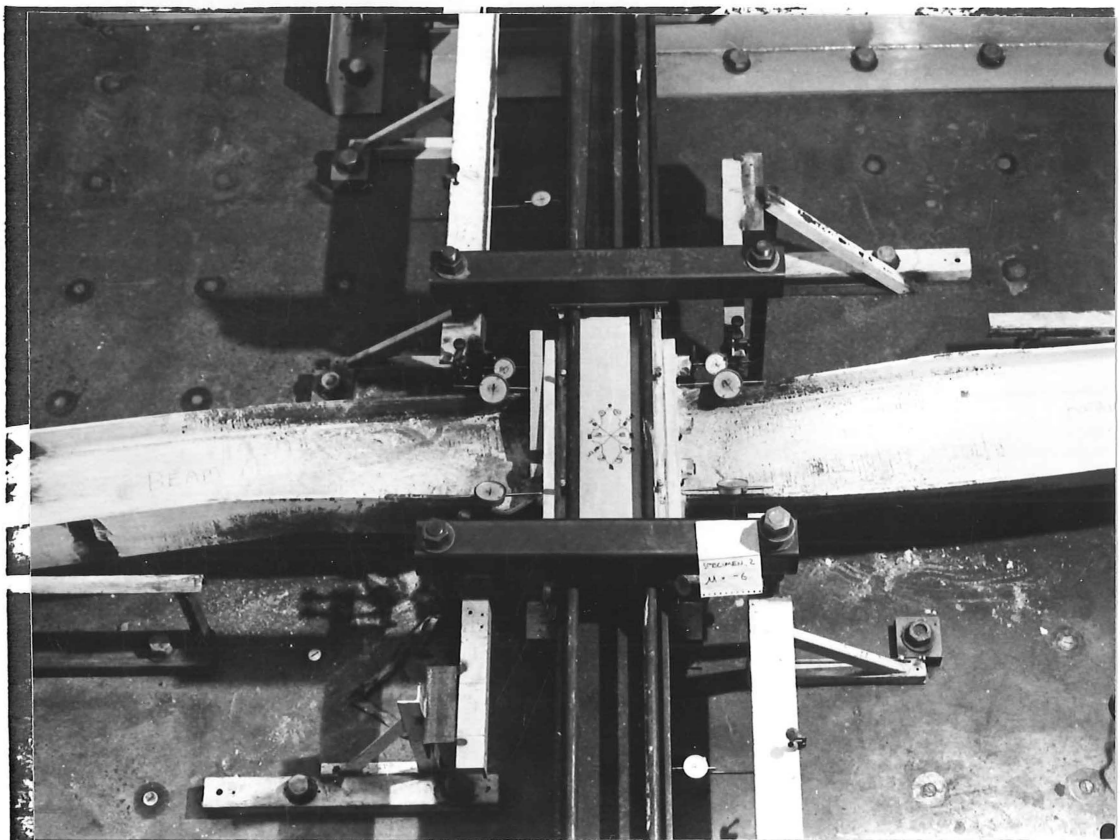


FIG. 5.2.7 General view of specimen two at $\mu = -6$.

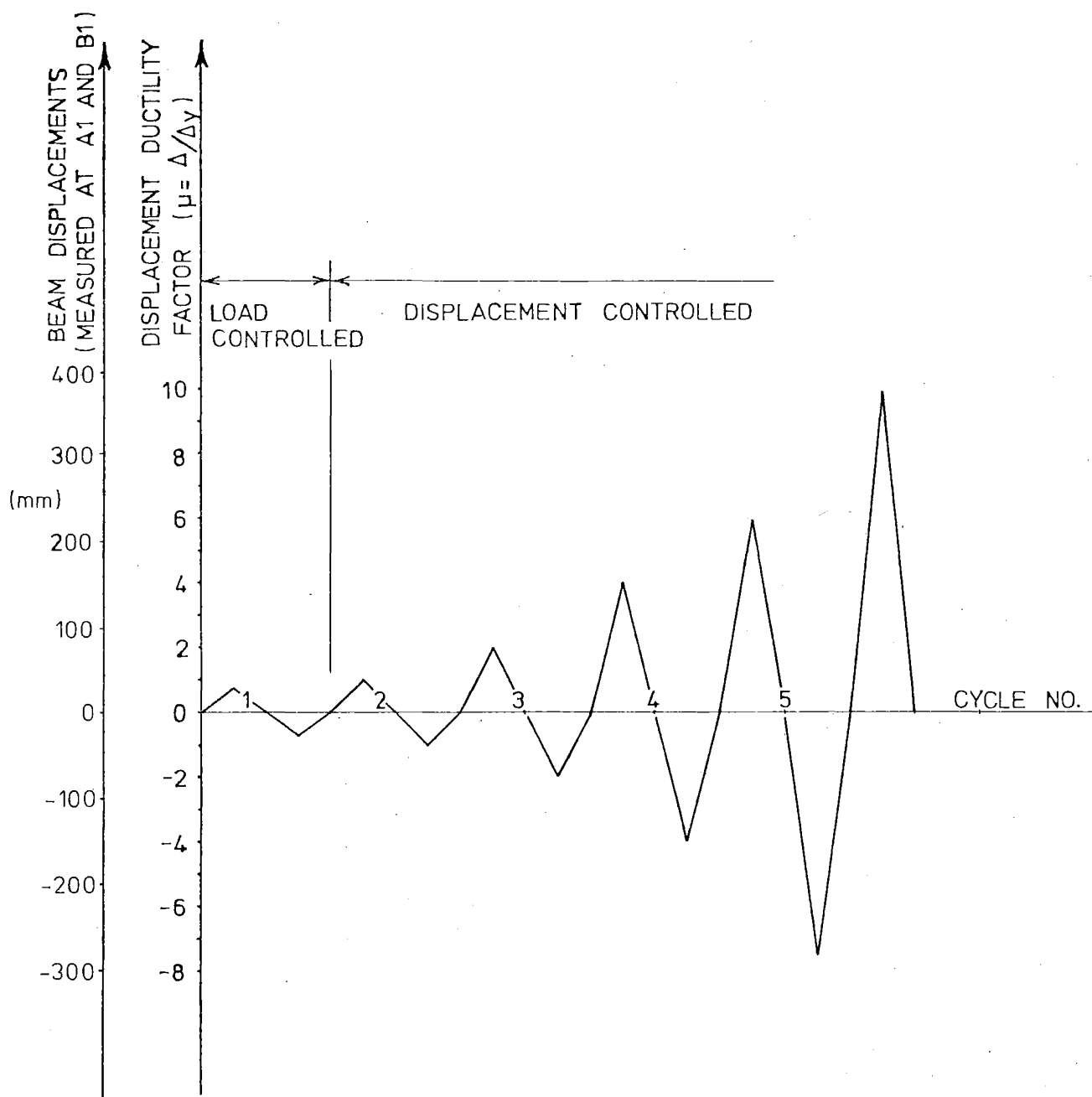


FIG. 5.3.1 Loading pattern, specimen three.

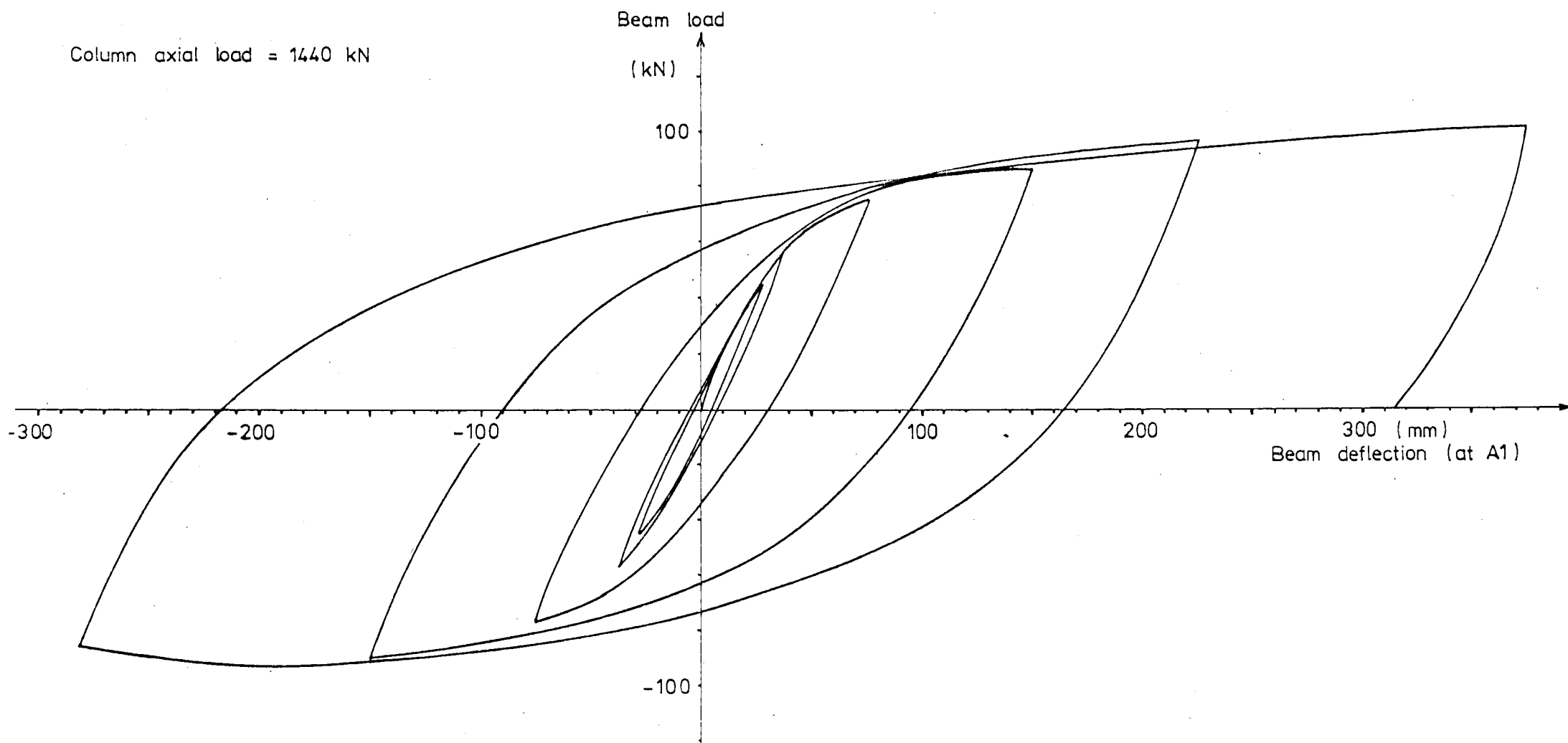


FIG. 5.3.2 Load versus deflection, beam "A", specimen three.

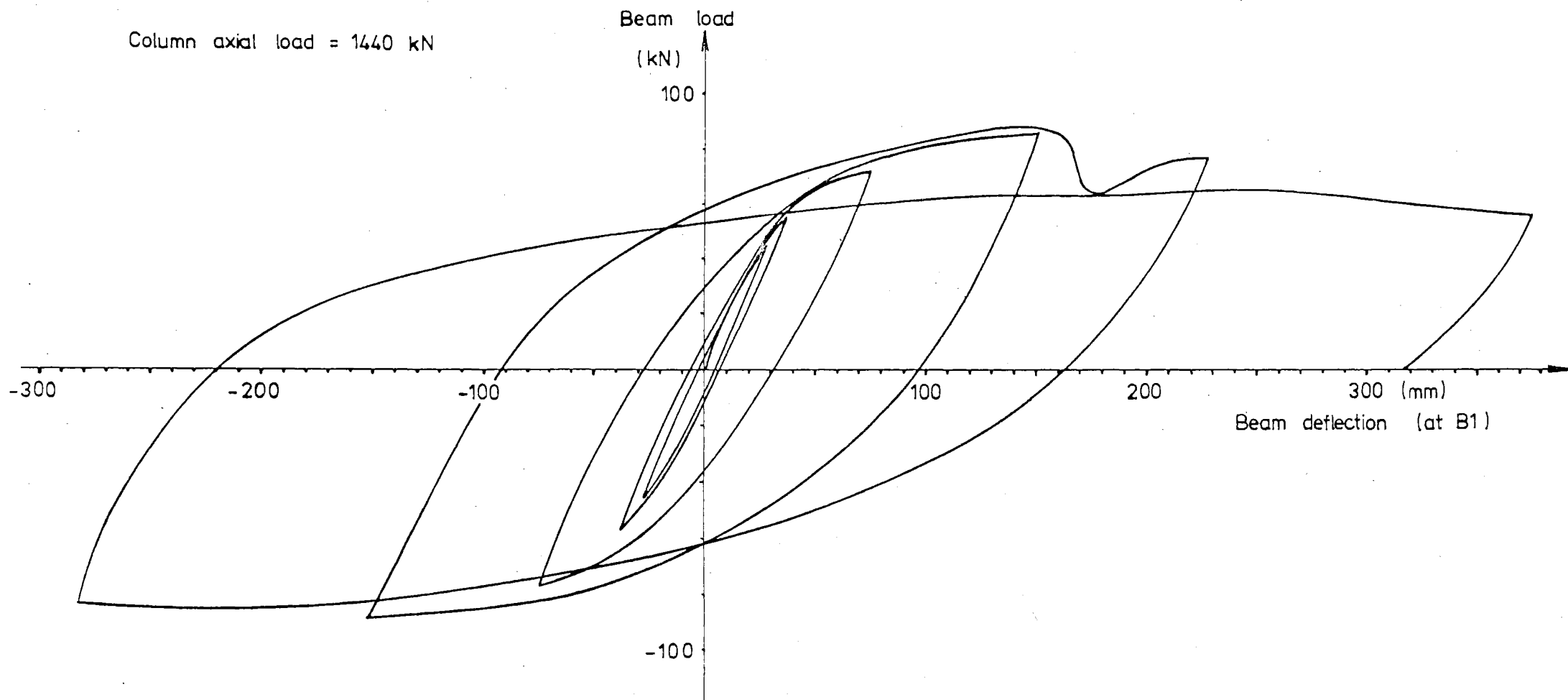
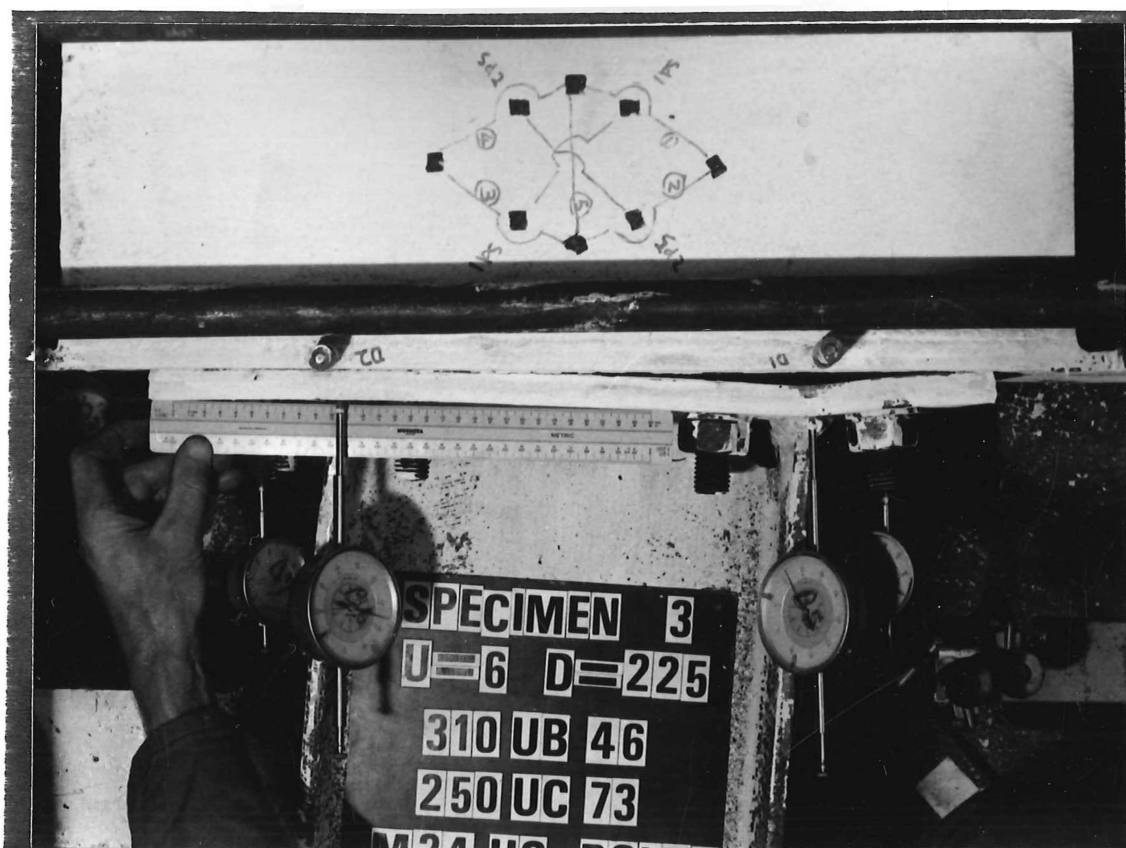
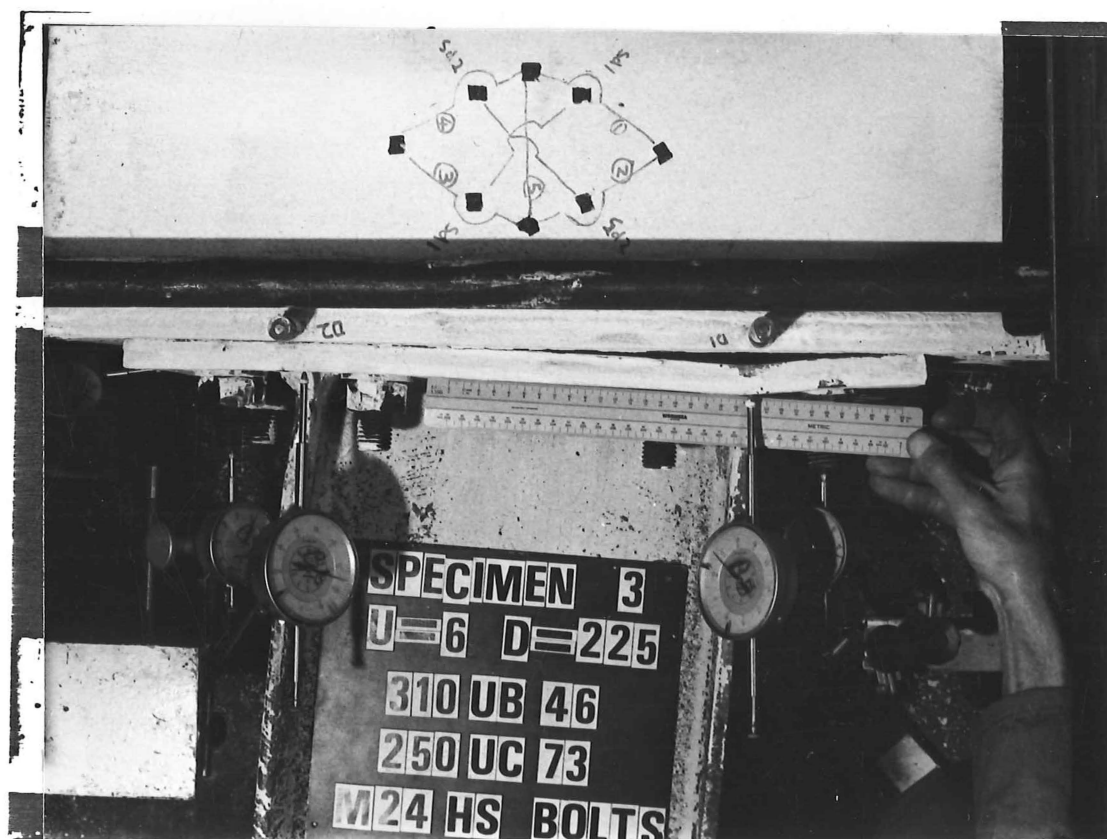


FIG. 5.3.3 Load versus deflection, beam "B", specimen three.



(a)



(b)

FIG. 5.3.4(a) and (b) End plate of beam "B", specimen two, when $\mu = +6$.

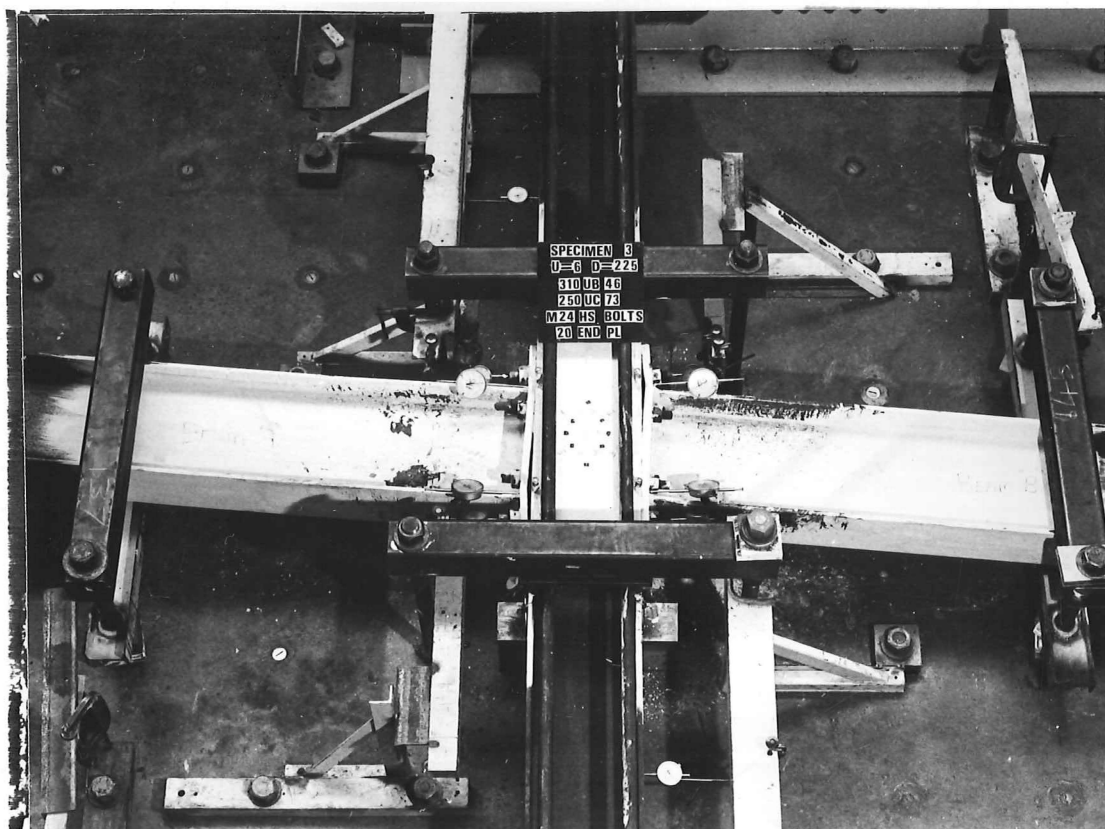


FIG. 5.3.5 General view of the connection, specimen three,
at $\mu = + 6$.

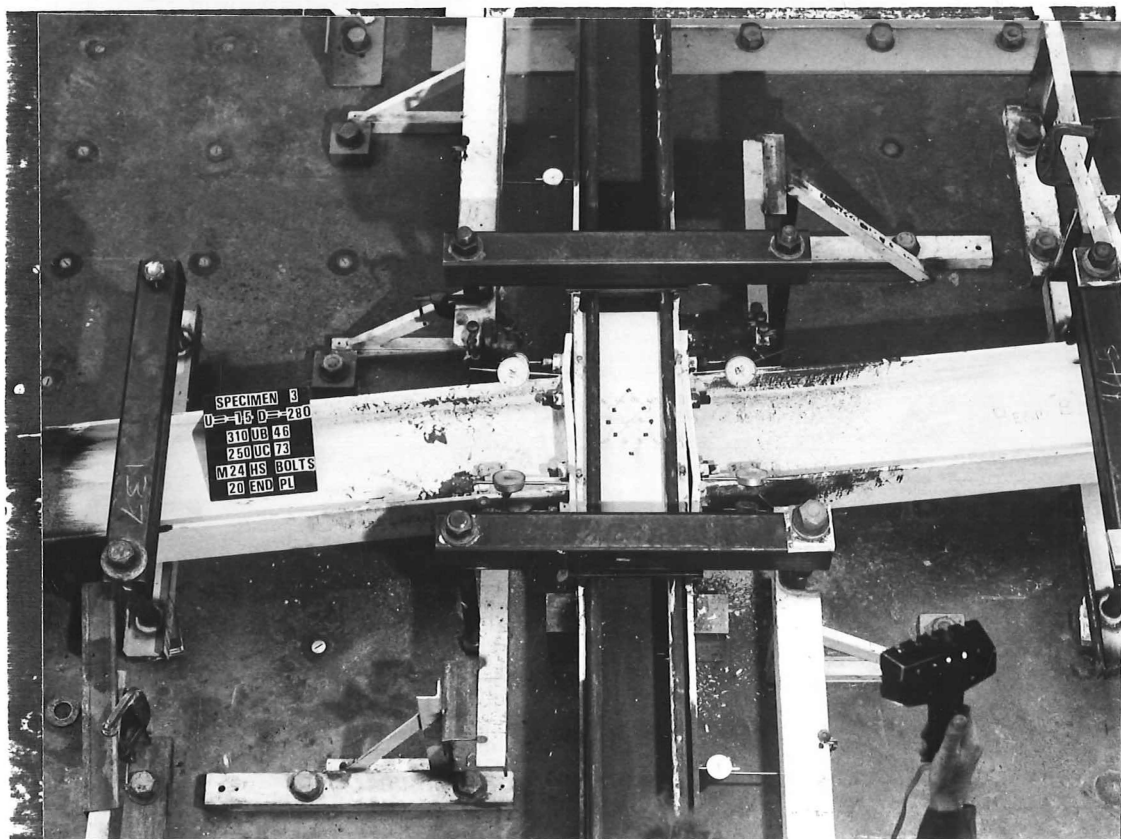


FIG. 5.3.6 General view of the connection, specimen three,
at $\mu = - 7.5$.

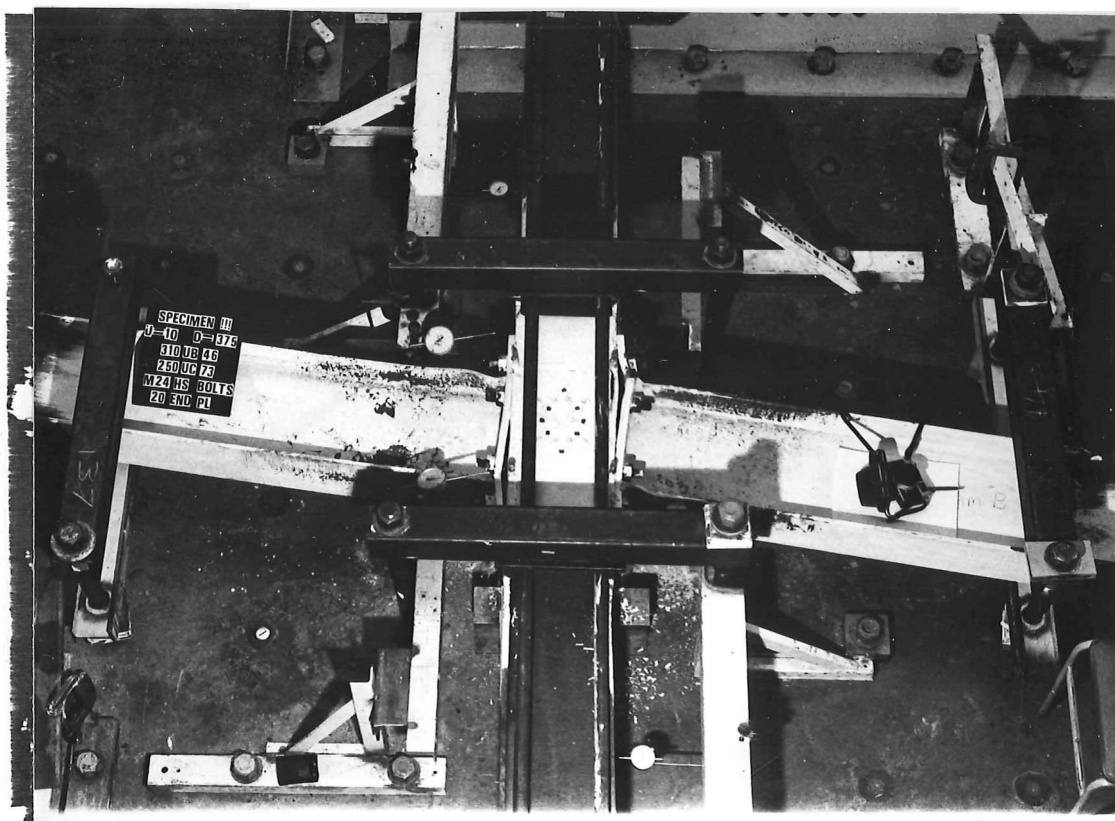


FIG. 5.3.7 General view of the connection, specimen three at $\mu = + 10$.

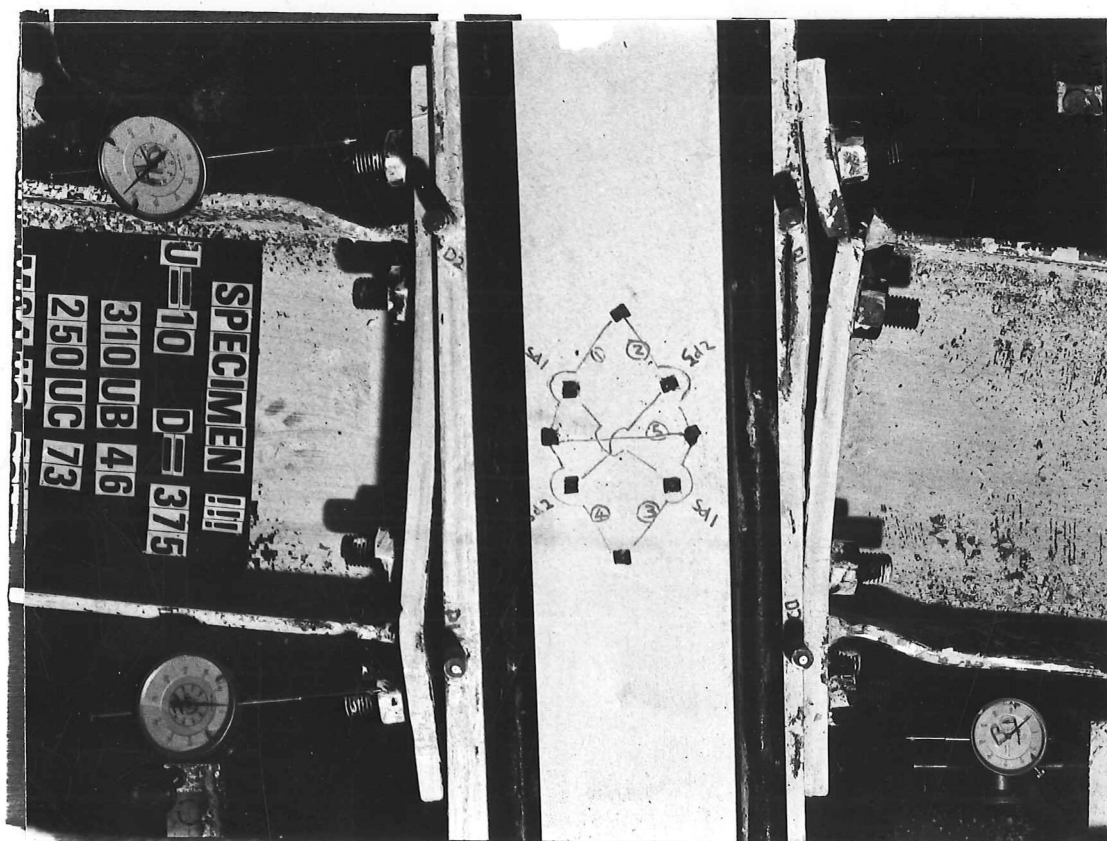


FIG. 5.3.8 Close up view of the connection, specimen three at $\mu = + 10$.



FIG. 5.3.9 Fracture in the end plate of beam "B", specimen three.



FIG. 5.3.10 Fracture in the end plate of beam "B" and some evidence of bending in double curvature in the end plate outstand, specimen three.



(a) Along the column.



(b) Across the column.

FIG. 5.3.11(a) and (b) Deformations of the column flange on the beam "A" side of specimen three.

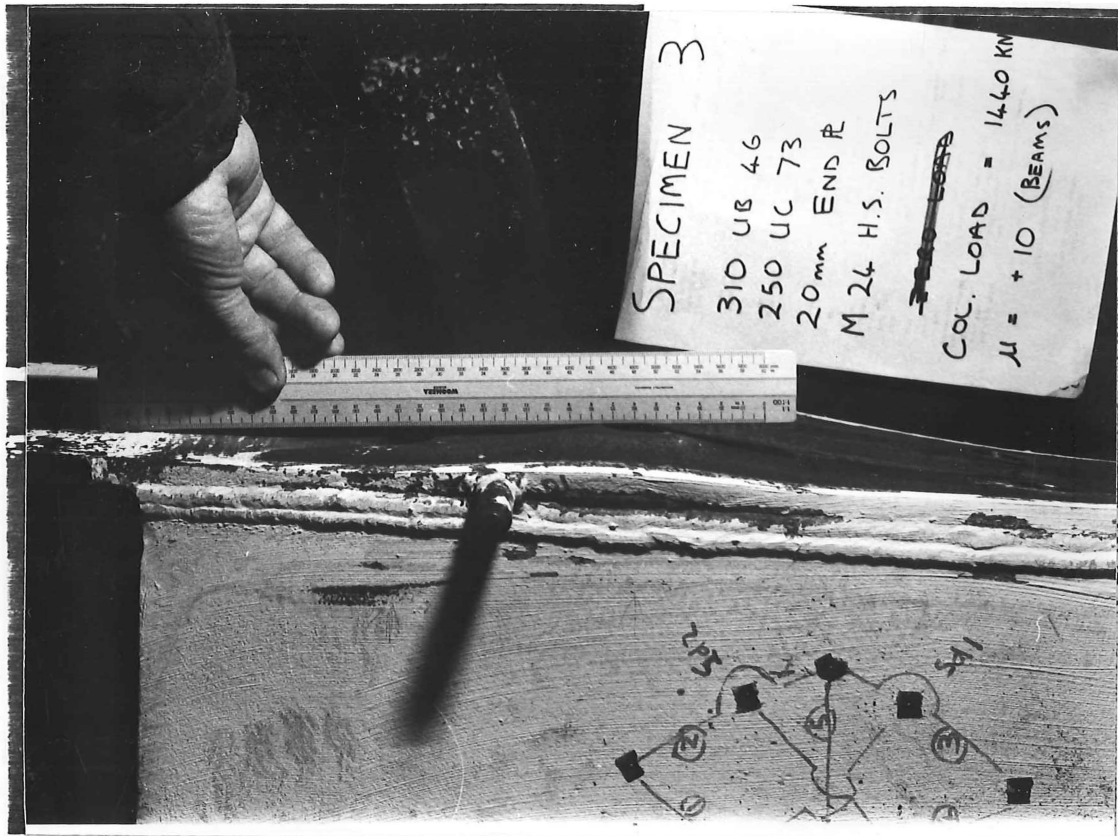


FIG. 5.3.12 Deformation of the column flange on the beam "B" side and partial fracture between the column flange and doubler plate butt weld, specimen three.

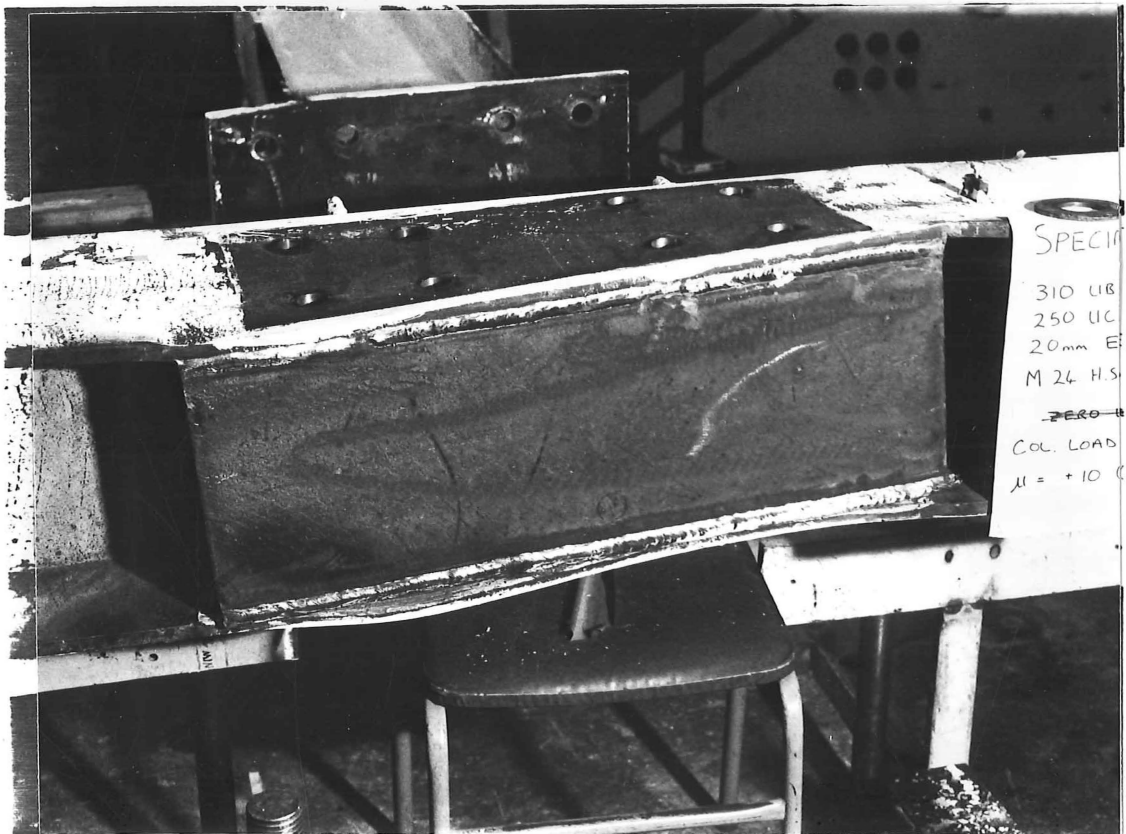


FIG. 5.3.13 View of panel zone where fracture has occurred over the full length between one of the column flanges and its doubler plate butt weld, specimen three. Beam "A" side as shown here is on top

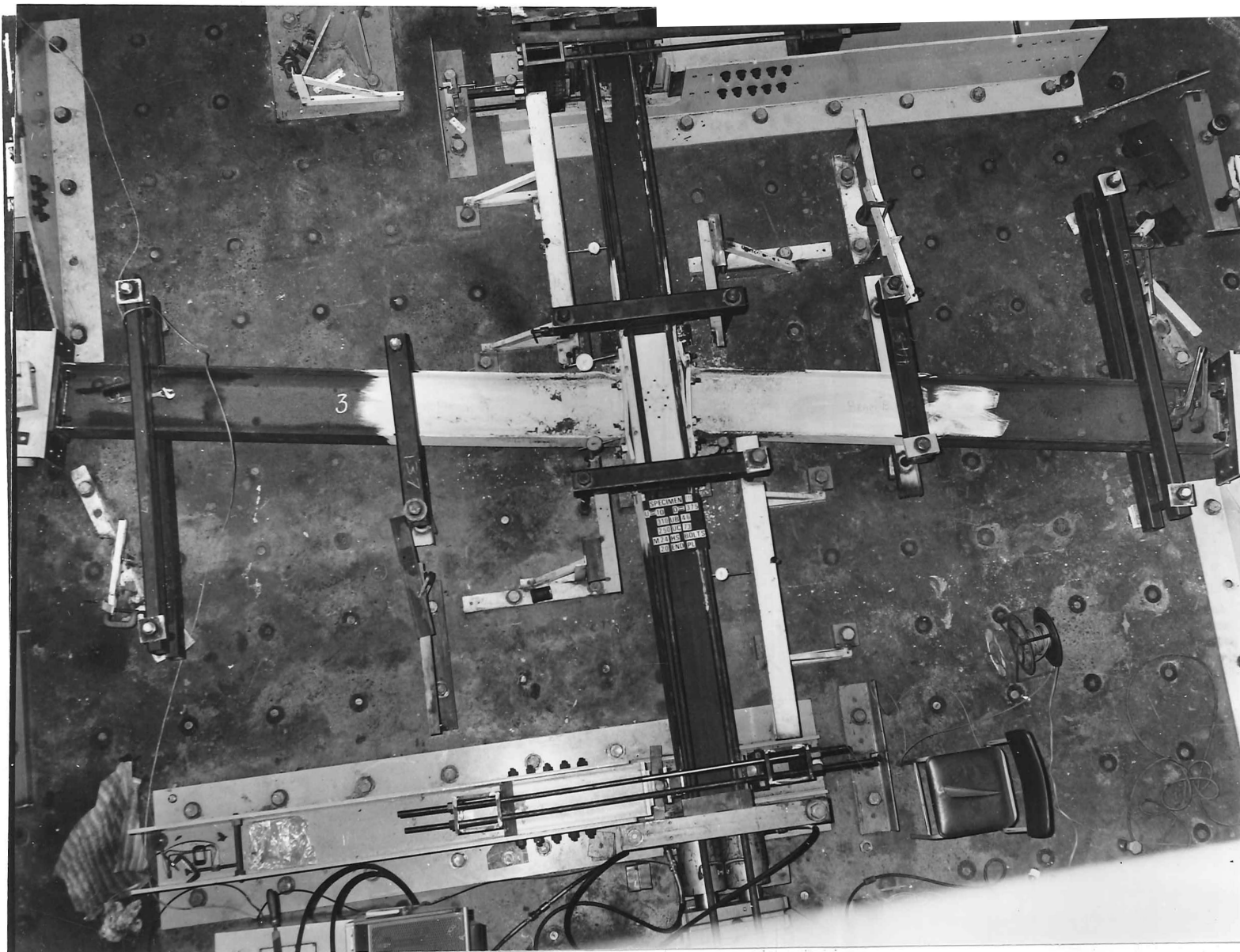


FIG. 5.3.14. General view of specimen three after the test showing additional beam bracing. c.f. Fig. 4.3 8

CHAPTER 6

DISCUSSION

6.1 INTRODUCTION

In these tests all three specimens were generally well behaved although a more detailed discussion on their performance and nature now follows.

Progressive yielding throughout the cyclic loading tests was only evident in the column where there was a constant axial column load with alternating bending moment and shear forces. The deformations in the beams, the end plates, and the lateral deformations in the column flanges were all cyclic in nature; i.e. all the inelastic displacements were completely reversed in the following half of the loading cycle. This meant that efficient use was made of the ductile characteristics of these components with respect to there being no progressive type of failure.

The connections in specimens one and two were strong enough to transmit beam actions and to encourage most of the inelastic deformation to occur in the beams. In specimen three the beam "A" side of the connection behaved very well with respect to its design strength. The beam "B" side however whilst it was strong enough to surpass its design strength it did not have the ductile characteristics in the end plate and possibly in the column flange stiffening to carry the ultimate load to as high a ductility as the beam "A" side.

In specimens one and two lateral bracing was provided for the beams at a distance of 2160 mm from the column face. Refer to Fig. 4.2. This satisfied the code⁽¹⁹⁾ requirements that the distance be less than,

$$\frac{960 \times \alpha \times r_y}{f_y}$$

For the beam size tested this distance was 2370 mm. Significant lateral bending and twisting had occurred when the tests one and two were stopped at approximately $\mu = 6$. They were stopped because of the magnitude of the in plane beam bending deformation. The beams were still able to carry high loads at this stage despite their apparent lateral deformations. Additional lateral bracing was used on specimen three to reduce these out of plane deformations, as shown in Fig. 4.2.

6.2 BOLTS

It was difficult to apply the exact bolt tightening procedure set out in the "Part turn" method⁽¹⁷⁾ because of welding distortions in the end plate and column flanges. This is because the ideal "snug tight" condition with all the joint surfaces in close contact could not be achieved without a significant bolt load from tightening. In specimens one and two the M30 H.S. bolts had enough strength as would have been expected from the load capacities as shown in the tables 1(b) and 2.

In specimen three the loads in the beam "A" bolts exceeded their design capacity without failure by a factor of 1.54. After fracture had occurred in the end plate of beam "B" the bolts just inside its tension flange had to carry a very large load. If it was assumed that no prying occurred here and that the lever arm opposing the beam moment was between the beam compression flange and the two tension bolts then the load on these bolts exceeded their design capacity by a factor of 1.7.

For this type of connection it seems to be a reasonable assumption that the load is shared equally among the four tension flange bolts because whilst the bolts inside the beam flanges carry more of the tension flange load, as indicated by Surtees and Mann⁽¹⁰⁾, the bolts outside it appear to be subjected to higher prying effects.

One feature that has not been considered much in the past and which was evident in these tests was the reduction in the prying effects due to the deformation of the column flanges. If these column flange deformations had not occurred then the bolt prying effects would have been larger, especially in specimens one and two where the "a" dimension in the end plate was small relative to the "b" dimension and the bolt size diameter "D".

The beam shear force in all three specimens was transferred across the interface between the end plate and the column flange predominantly by friction. This was deduced from the fact that there was no significant relative sliding movements. If the shear force was carried partly by bearing in the bolts then large sliding movements, say 1 to 2 mm, would have been detected in the dial gauges "A3" and "B3" as the bolt hole clearances were taken up in the shear force direction. If the connection in specimens one and two had been designed to carry the shear force by friction in the beam compression flange region the corresponding design capacity⁽¹⁷⁾ for shear around the four M30 H.S. bolts would have been 382 kN. This is more than the 84 kN actually designed for. Similarly the design shear capacity in friction of specimen three in the region of the four M24 H.S. compression flange bolts was 241 kN which was also higher than the shear force resistance required. It should be remembered however that a relatively larger beam shear force would have eventuated if either a shorter beam span or a deeper beam section had been used.

6.3 END PLATE

The portion of the end plate outside the beam tension flange did not deform in double curvature to the extent that was initially assumed. This is because the deformation of the column flange as shown in Fig. 5.3.11(a) relaxed the constraints that encourage the end plate outstand to develop a reverse curvature in itself. Subsequently most of the inelastic deformation that occurred in the end plate was concentrated in the area immediately adjacent to the beam tension flange as is shown in Fig. 5.3.4. However it appears that the outstand portion of the end plate was still capable of carrying a reasonable load. This was probably because a significant amount of elastic double curvature occurred throughout the test. In the design of the end plate most of the equations recommended assume that a yield line develops along the horizontal line of the bolt's centres in the end plate outstand. This yield line was not obvious here but that assumption would still be legitimate as long as the column flanges were stiff enough and the end plate dimensions, in particular "a", were adequately proportioned. This would be to encourage the moment along the mentioned line to reach yield even though no further curvature ductility may have been achieved there.

The recommendation by Mann and Morris⁽¹⁾ that "a" should be not less than 2.5 times the bolt diameter appears to be very sensible. The dimension "a" used in specimen three was 60 mm which was exactly 2.5 times the bolt diameter, 24 mm, used. In specimens one and two "a", 50 mm, was less than the 2.5 times 30 mm. Subsequently this would have reduced the effective bending in double curvature of the end plate outstand. Another reason for keeping "a" large is that a smaller column flange mechanism might otherwise occur as discussed later in this chapter which would similarly reduce the prying effects and bending in double curvature.

The end plate inside the beam flanges seemed to behave generally in the way that was predicted by Surtees and Mann.⁽¹⁰⁾ This was perhaps most obvious after fracture had occurred in the beam "B" end plate of specimen three. After this fracture had formed the bolts and end plate immediately inside the beam tension flange were able to support a beam moment of 70% of what it was immediately prior to the fracture event. This decrease in load carrying capacity is shown in Fig. 5.3.3 and indicates that the larger portion of the beam tension flange force was carried by the end plate immediately inside that flange. Close inspection of that end plate in the region between the beam flanges after testing showed that it had deformed in much the same way as that assumed by Surtees and Mann.⁽¹⁰⁾ Refer to Fig. 3.3. In particular the deformation in the end plate due to the restraining effect of the beam web went to zero at the mid depth of the beam as was assumed⁽¹⁰⁾ in Fig. 3.3.

One variable that Surtees and Mann's⁽¹⁰⁾ equation,

$$t = \left[\frac{M_B}{d_f \times f_{yp} \times \left(\frac{2B}{C} \right) + \frac{d_f}{A}} \right]^{\frac{1}{2}}$$

does not include is the thickness of the beam flange and the thickness of the welds, e.g. fillet welds or butt welds. It was apparent throughout the tests that the end plate deformations around the beam tension flange were quite sensitive to the magnitude of "b". This appears to be the reason why the specimen one butt welded end plates deformed more than the specimen two fillet welded end plates and why in specimen three prior to fracture in the beam "B" end plate the deformations in the beam "B" end plate, which had the more largely splayed butt welds, were comparatively less than those in the beam "A" end plate. Mann and Morris⁽¹⁾ do appear

to use "b" as being measured between the bolt centres and the edge of the adjacent weld in their equation,

$$t = \left(\frac{M_B \times b}{d_f \times f_{yp} \times B} \right)^{\frac{1}{2}}$$

The fracture in the specimen three beam "B" end plate occurred in an area of high stress concentration. These stresses were due to bending in the end plate and tension from the beam tension flange. The magnitude of these stresses was thought to have been increased by the close proximity of the bolts to the beam tension flange. Their close proximity may have prevented the stresses from dispersing more evenly across the end plate width. The distance "b" measured from the bolt centres outside of the beam flange to the edge of the adjacent weld was 30 mm in the area where the fracture occurred and was between 35 and 38 mm at the other three end plates to beam flange junctions. It seems that the curvature ductility demand was greater in the end plate immediately outside of the beam tension flange than it was immediately inside it. This was largely due to the restraint of the beam web on the end plate and the relative rotation between the column face and the end plate, (in the plane of the beam and column centrelines). Perhaps a more realistic values of "b" would have been achieved for specimen three if "b" had been detailed for the erection clearances necessary with standard impact wrenches⁽²⁰⁾ and/or if better quality control had been executed during fabrication to avoid off set end plates and largely splayed butt welds.

6.4 COLUMN FLANGES

In these three specimens two different types of column flange stiffening were used. The first and more conventional type used in specimen one resulted in some significant welding distortions although it would probably have still been acceptable in practice. The second type of stiffening tested here in specimens two and three was more easily fabricated and resulted in only relatively small welding distortions.

The column flanges of specimens one and two were both designed to be stronger than the adjacent beams. This was perhaps the main reason why they performed safely with very little deformation during their tests.

In specimen three the column flange tip stiffening system was underdesigned to encourage it to fail. It performed well on the beam "A" side but failed on the beam "B" side although only at a later stage in the test. The ultimate load reached on the beam "A" side was 1.6 times the design yield capacity of the column flange. Results of a yield test on a column flange sample indicated that it had an ultimate tensile strength of 1.54 times the yield strength. With this in mind and considering that the "upper bound" yield line method of calculating the design yield capacity was already theoretically unconservative, especially when it had neglected the existence of other column flange stresses, it seemed that the column flange on this side of the column performed very well. Some additional strength may have been imparted to it by the clamping action of the bolt head and nuts. If this clamping action was significant its influence on the column flange yield mechanism would have probably been only in the area immediately around the bolts rather than on the mechanism as a whole. This subject of the clamping effects in this type of situation has been briefly discussed⁽¹⁵⁾ but there does not appear to have been much research in this area. In this clamping type of action the bolt load was probably exerting an approximate hexagonal line load rather than the assumed point load. This would have certainly increased the theoretical design capacity of the column flange.

On the beam "B" side the column stiffening system failed when fractures occurred in it as was described in Chapter Five. Before the fractures occurred the load on the beam reached a level which exceeded the corresponding design yield capacity of the column flange by a factor of 1.4. This failure between the doubler plate butt weld and the column flange tip would in a normal situation be unacceptable because it severs the bulk of the shear strength in the panel zone. This would probably then lead to failure within the column at the connection. The line along which these fractures occurred was a line of high stress concentration. The stresses came from bending due to the column flange mechanism, tension or compression in the doubler plate resulting indirectly from the beam tension or compression flange, and longitudinal shear that was transferred between the column flanges and the doubler plates. It is possible that these fractures were initiated by the premature failure in the beam "B" end plate. This failure may have caused a larger load to be put on the column flange mechanism around the bolts that were just inside the beam tension flange. In this specimen the end plates and column flanges were under designed with respect to the beam

loads placed on them. In a normal design situation this type of column stiffening may be quite acceptable as was generally indicated by specimen two. It seems unlikely that it would have fractured if the beam end plate had not done so first and if the loads were lower.

In specimens one and two, where the end plate dimension "a" was only 50 mm, it appeared that the effect of prying between the end plate and the column flange may have had an influence on the yield line pattern in the column flange. This is perhaps another good reason for using the criterion suggested by Mann and Morris⁽¹⁾ to ensure that a reasonably large value of "a" is used.

The equations for determining the capacity in the column flanges, as given in Section 4.2, neglected the effects of other column flange stresses due to column axial load and bending. The capacities of the column flanges were sufficient in these tests but it is possible that problems could have been encountered if higher column axial loads and/or bending moments had been used. These longitudinal column flange stresses may not be too critical in earthquake loading situations because the column flange stresses due to bending tend to cancel out those due to axial compression in the beam tension flange region.

6.5 GENERAL DISCUSSION

In all these bolted end plate type beam to column connections it is important to extend the column web doubler plates beyond the boundaries of the column flange mechanisms.

These connections can be used for joining larger beam and column sizes but some problems can arise in the bolting aspect of the connection. With bigger beam sections larger beam tension flange forces have to be dealt with. Larger bolt sizes, i.e. M30 and M36 H.S. bolts appear to be uncommon in practice because of difficulties in tightening them.

Grundy et al⁽⁶⁾ suggested the use of eight bolts per beam tension flange but with the proviso that horizontal column flange stiffening be provided at the level of the beam flanges. Not much research seems to have been done into the actual load distribution between the eight bolts around that beam tension flange. Intuition would perhaps suggest that

whilst the four bolts outside the flange would share their loads reasonably evenly, the loads in the bolts inside the beam tension flange would tend to be nonuniform with more load being carried by the two centre bolts. This is because of the restraining effect of the beam web on the end plate. Similarly the restraining effect of the column web would attract more load towards the bolts that are closest to the column web both above and below the beam tension flange. . Perhaps to more evenly distribute the bolt loads the two bolts inside the beam tension flange and closest to the beam web could be moved further away from that beam flange.

Another method that can be used to reduce the beam tension flange force whilst still carrying a large moment in the beam is to haunch the beam at the connection.

CHAPTER 7

RECOMMENDATIONS FOR FURTHER RESEARCH

Some aspects about the behaviour of these connections that would probably benefit from further research are described in the following paragraphs.

The use of lower design loads for the bolts may result if a better understanding was developed for the criteria that governs the magnitude of those loads especially when the column flange is deforming and reducing prying effects.

Surtees and Mann's⁽¹⁰⁾ end plate thickness equation appears to be generally a lot less conservative than other similar equations. They do not appear to discern between fillet and butt welds which appear to make a difference to the end plate strength. A more structurally accurate solution may result if this variable were included in their equation. Some further cyclic loading tests of end plates to substantiate their load and stiffness characteristics would be helpful to confirm the validity of their equation for earthquake loading conditions.

The use of eight bolts per beam flange offers a way by which larger beam and column sizes can be joined by this type of connection. The main problem here is generally the lack of knowledge on the way the loads and stresses are distributed throughout the beam end plate, bolts and column flanges. The two main variables affecting this are the bolt positions and the column flange stiffening used.

CHAPTER 8

CONCLUSIONS

Three bolted end plate beam to column connections were tested here. The first two were designed to comply with the NZS 3404:1977. This was done by using the equations set out in Section 4.2 of this thesis and assuming a beam strain hardening factor of 25%. The third connection was underdesigned so that its behaviour at ultimate could be more closely studied.

1. In the first two tests the connections were able to support the ultimate plastic hinge beam loads in a relatively stiff manner.
2. In the third test the connections underwent larger ductile deformations at relatively higher loads without any strength degradation until later in the test when partial failure was initiated by fracture in the end plate.
3. The tests indicated that the beams needed laterally restraining by at least the amount required by the Standard AS 1250:1975 if higher ductilities were to be achieved in the beams.
4. The tests carried out here have not been able to cover a wide range of these connections but their results indicate that these connections can be designed and fabricated to reliably withstand reversed cyclic ultimate beam loads.

REFERENCES

- (1) Mann, A. P., and Morris, L. J., "Limited Design of Extended End-Plate Connections". Journal of Structural Division, ASCE, ST3, March 1979, pp 511-526.
- (2) Packer J. A., and Morris, L. J., "A limit state design method for the tension region of bolted beam/column connections". The Structural Engineer, October 1977, No.10, Volume 55, pp 446 - 458.
- (3) Fisher, J. W., and Struik, J. H. A., "Guide to Design Criteria for Bolted and Riveted Joints", 1974, John Wiley & Sons.
- (4) "Plastic Design in Steel - A Guide and Commentary", Manual No. 41, ASCE, 1971, New York.
- (5) Sherbourne, A. N., "Bolted Beam to Column Connections", The Structural Engineer, June 1961, Volume 39, pp 203-210.
- (6) Grundy, P., Thomas, I. R., and Bennetts, I. D., "The Design of Beam to Column Moment Connections using End Plates and High Strength Bolts", AISC Second Conference on Steel Developments, Australian Institute of Steel Construction, May 1977, Melbourne, pp 76-84.
- (7) "Standardised Structural Connections", AISC, Australian Institute of Steel Construction, Hogan, T. J., Thomas, I. R., 1978.
- (8) Douty, R. T., and McGuire, W., "High Strength bolted Moment Connections", Journal of the Structural Division, ASCE, Vol.91, No.ST2, April 1965, p.101.
- (9) Nair, R. S., Birkemoe, P. C., and Munse, W. H., "Behaviour of Bolts subject to Tension and Prying", Journal of the Structural Division, ASCE, Vol.100, No.ST2, February 1974, p.351.
- (10) Surtees, J. O., and Mann, A. P., "End-Plate Connections in Plastically Designed Structures", Conference on Joints in Structures, Vol.1, Paper 5, University of Sheffield, England, July, 1970.

- (11) Zoetemeijer, P., "A Design Method for the Tension side of Statically Loaded, Bolted Beam to Column Connections", Heron 20, No.1, Delft University, Delft, The Netherlands, 1974.
- (12) "E.C.C.S. Recommendations for Steel Construction", European Convention for Constructional Steelwork, 1977.
- (13) Mann, A. P., "Plastically Designed End-Plate Connections" thesis presented to the University of Leeds, at Leeds, England in 1968, in partial fulfilment of the requirements for the degree of Doctor of Philosophy.
- (14) Graham, J. D., Sherbourne, A. N., Khabbaz, R. N., and Jensen, C. D., "Welded Interior Beam-to-Column Connections", AISC, New York, 1959.
- (15) Surtees, J. O., Howlett, J. H., Hairsine, R. C., Correspondence on "A limit state design method for the tension region of bolted beam-column connections", Packer, J. A., and Morris, L. J., Ref.(2), The Structural Engineer, August 1978, No.8, Vol.56A, pp 217-223.
- (16) N.Z.S. 3404-1977, "Code for Design of Steel Structures".
- (17) AS 1511-1973. "High Strength Structural Bolting Code".
- (18) Gorenc, B. E., Tinyou, R., "Steel designers handbook", 1976.
- (19) AS 1250 - 1975, "SAA steel structures code".
- (20) Australian institute of steel construction (AISC), "Safe load tables for structural steel", third edition.
- (21) NZS 4203:1976, Code of practice for "General Structural Design and Design Loadings for Buildings".
- (22) AS 1391-1974, "Methods for tensile testing of Metals".

APPENDIX I

DERIVATION OF COLUMN FLANGE CAPACITY

This derivation is specifically for the situation where the column web doubler plates are full strength butt welded to the column flange tips. Dimensions and symbols used in this derivation may be found in Fig's 4.9 and 4.10 and in the Notation. This derivation is based on yield line theory and so will theoretically only provide an upper bound solution.

Assumptions are:

- (1) That the panel zone doubler plates on the column flange tips are stiff enough (thick enough) to cause the full plastic moment to be reached in either the doubler plate or the column flange on the line AD, see Fig's (4.9) and (4.10).
- (2) That the effect of stresses due to the column axial load and bending may be neglected. Allowance could be made for the existence of these by using appropriate reduced plastic moment capacities in the yield lines that extend across the column flanges.

(A) For the yield line pattern shown in Fig. 4.9.

If the yield line, EF is displaced through a distance d' then:

The work done by $0.5 \times F_{mp}$ is,

$$W_E = 0.5 \times F_{mp} \times d'$$

The work done by the hinge mechanism is,

$$W_I = \sum M \theta L$$

using $M = \frac{f_{yc} \times T_c^2}{4}$

and $r = \frac{T_p^2}{T_c^2}$ when $T_p^2 < T_c^2$

or $r = 1$ when $T_p^2 > T_c^2$

$$W_I = M \times \left(\frac{2d' (m+n)}{g} + \frac{d' (2g+C)}{m} + \frac{d' (2g+C) r}{n} + \left(\frac{d'}{m} + \frac{d'}{n} \right) (C - D') \right. \\ \left. + d' \left(\frac{m - 0.5D'}{g} + \frac{g - 0.5D'}{m} \right) + d' \left(\frac{n - 0.5D'}{g} + \frac{g - 0.5D'}{n} \right) \right)$$

$$\frac{dW_I}{dg} = 0.$$

$$\therefore g = \left(\frac{mn (3m + 3n - D')}{3n + (1+2r)m} \right)^{\frac{1}{2}}$$

putting $W_E = W_I$

$$\text{then } F_{mp} = T_c^2 + f_{yc} \left(\frac{3m + 3n - D'}{2g} + \frac{3g + 2C - 1.5D'}{2m} + \frac{g(1+2r) + (1+r)C - 1.5D}{2n} \right)$$

(B) For the yield line pattern shown in Fig. 4.10

If the point E is displaced through a distance d' then the work done by $0.25 F_{mq}$ is,

$$W_E = 0.25 F_{mq} \times d'$$

The work done by the hinge mechanism, " W_I ", is,

$$W_I = M d' \left(\left(\frac{m - 0.5D'}{g} + \frac{g - 0.5D'}{m} + \frac{n - 0.5D'}{g} + \frac{g - 0.5D'}{n} \right) \times 2 + \frac{2(m+n)}{g} + \frac{2g}{m} + \frac{2g}{n} \right)$$

$$\frac{dW_I}{dg} = 0 \quad \therefore g = \text{as for } F_{mp}$$

$$\therefore F_{mq} = 2 T_c^2 \times F_{yc} \left(\frac{2m + 2n - D'}{g} + \frac{(2g - 0.5D') (m+n)}{mn} \right)$$